

Hartree-Fock Computation of the High- T_c Cuprate Phase Diagram

R. B. Laughlin

Department of Physics, Stanford University, Stanford, CA 94305*

(Dated: January 21, 2014)

A computation of the cuprate phase diagram is presented. Adiabatic deformability back to the density function band structure plus symmetry constraints lead to a Fermi liquid theory with five interaction parameters. Two of these are forced to zero by experiment. The remaining three are fit to the moment of the antiferromagnetic state at half filling, the superconducting gap at optimal doping, and the maximum pseudogap. The latter is identified as orbital antiferromagnetism. Solution of the Hartree-Fock equations gives, in quantitative agreement with experiment, (1) quantum phase transitions at 5% and 16% p -type doping, (2) insulation below 5%, (3) a d -wave pseudogap quasiparticle spectrum, (4) pseudogap and superconducting gap values as a function of doping, (5) superconducting T_c versus doping, (6) London penetration depth versus doping, and (7) spin wave velocity. The fit points to superexchange mediated by the bonding O atom in the Cu-O plane as the causative agent of all three ordering phenomena.

I. INTRODUCTION

The purpose of this paper is to discuss the theoretical phase diagram for the high- T_c cuprate superconductors shown in Fig. 1¹⁻⁸. It is generated using standard Hartree-Fock methods starting from a Fermi liquid theory with three interaction parameters⁹⁻¹¹. It is characterized by three interpenetrating order parameters: spin antiferromagnetism, or spin density wave (SDW), d -wave superconductivity (DWS) and orbital current antiferromagnetism, or d -density wave (DDW)¹²⁻¹⁴.

However, the central issue of the paper is not building better models for the cuprates but the application of elementary quantum mechanics to them. The equations that generate Fig. 1 are not just made up. They are the *only* equations one can write down that are compatible with adiabatic evolution out of a fictitious metallic parent, plus a handful of experimental fiducials. This evolution, which strictly enforces the Feynman rules, is the starting point of all conventional solid state physics. The ability of these equations to account broadly and well for all key aspects of high- T_c phenomenology thus indicates that high- T_c cuprates are *not* qualitatively different from other solids, as has often been suggested might be the case, but are simply materials with unusually complex low-energy spectroscopy. This complexity, which results from delicate interplay of multiple order parameters, has prevented the problem from being solved empirically. But elementary quantum mechanics so circumscribes the mathematics that one can say with confidence that the phase diagram in Fig. 1 is correct, even though one of its features, the identification of DDW with the cuprate pseudogap, is still in doubt phenomenologically¹⁵⁻¹⁹.

The results reported in this paper therefore have significance far greater than simply accounting for the behavior of a particular class of materials. The 25-year history of the cuprates has demonstrated rather brutally that first-principles theoretical control of solids at the energy scales relevant to electronic transport does not exist. This is so even though the underlying Hamiltonian of conventional matter is known exactly. Computers

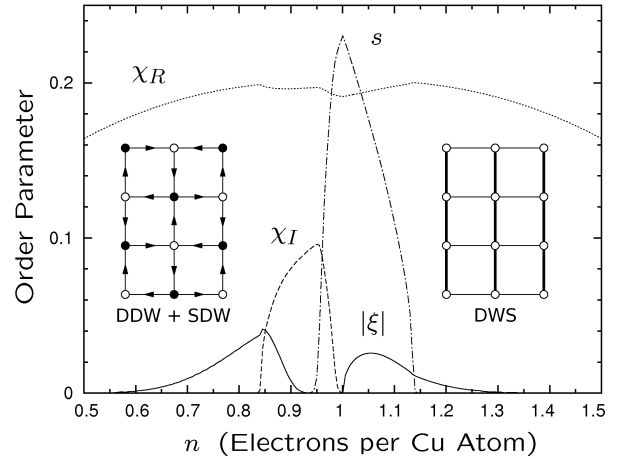


FIG. 1: Zero-temperature phase diagram of the Hamiltonian $\mathcal{H}_0 + \Delta\mathcal{H}$ defined by Eqs. (2) and (3) for the case of $U = 0.76 t$, $J = 0.75 t$, $V_c = 0.87 t$, $t' = 0.1 t$, and $V_n = V_t = 0$. The order parameters s , χ_I , and ξ are defined by Eqs. (5). The self-consistency conditions are Eqs. (32) - (36). The insets show the sense of the signs for spin and orbital current antiferromagnetism (left) and d -wave superconductivity (right). The system insulates everywhere s is nonzero.

were not able to solve this problem. It was too hard for them. One obtains control, if at all, only by exploiting the universal low-energy properties of quantum phases. The simple equations that describe these properties are the starting point for predictive computation. The practice of adiabatically evolving from fictional parent vacua is precisely what distinguishes solid state physics from materials chemistry, and is what makes it so much more powerful than the latter as a basis of engineering.

Historical Background

The discovery of high- T_c cuprate superconductivity revealed that standard methods for computing the prop-

erties of solids were more seriously flawed than previously thought^{20–24}. On the one hand, the materials in question were sufficiently conventional chemically that they should have yielded to ordinary self-consistent band structure analysis²⁵. The latter requires them to be metals in the absence of translational symmetry breaking. On the other, their phenomenology was totally incompatible with the conventional theory of metals²⁶. Not only were their superconducting transition temperatures higher than existing theory said was possible without structural instability, their transport phenomenology was wildly irregular, and the violent variation of the superconducting transition temperature and superfluid density had no precedent^{27–29}.

Accordingly, Anderson and others suggested at the time that cuprate superconductivity might be an important new aspect of Mott insulation, an equally serious conceptual issue that had emerged 40 years earlier^{30–32}. This proposition was, and still is, extremely radical. Its central premise is that standard practices of solid state physics based on the adiabatic principle are irrelevant to these materials³³. Nonetheless it has now become mainstream and central to the field, in part because so many experiments have defied conventional explanation. It has also given rise to a number of related non-adiabatic theoretical ideas such as the non-Fermi liquid state, the holographic metal and the orthogonal metal^{34–39}.

Unfortunately, the phenomenological definition of a Mott insulator has always been somewhat difficult to state and is sometimes expanded to include the entire class of ordinary magnetic insulators⁴⁰. The underlying idea is of a system that insulates when it ought not to. Thus the spin-unpolarized band structures of the transition metal monoxides FeO, CoO, and NiO are metallic but the materials themselves are all good insulators^{41,42}. CoO has an odd number of electrons per unit cell. All three oxides possess antiferromagnetic order at zero temperature, which doubles the unit cell and thus formally allows them to insulate by the usual rules of band structure^{43–45}. However, the strength of conventional exchange is inadequate to cause insulation in this way except in NiO, and all three materials continue to insulate above their Neél temperatures. Other materials typically (but not always) categorized as Mott insulators include MnO, V₂O₃, Fe₂O₃, LaTiO₃, Y₂Ru₂O₇, YTiO₃, YVO₃, and Sr₂VO₄^{46–53}. The majority of identified Mott insulators are transition metal oxides.

The enormous amount of theoretical work stimulated by the cuprate discovery has now built up a strong case that the Mott insulator does not exist as a distinct zero-temperature state of matter. This was arguably unclear when the cuprates were first discovered, but it is no more. Two decades of intense focus on the problem have not led to a single instance of an actual wavefunction for a Mott insulator written down in terms of the underlying electron coordinates^{54–58}. The resonating valence bond state of Anderson appears to be a counterexample, but this is not so^{59,60}. It is actually a *d*-wave superconductor. It is

made by adding a short-range Coulomb repulsion to a superconducting Hamiltonian and then taking the strength of this repulsion to large values while legislating that no phase transition occurs⁶¹. Were such a perturbation actually applied without the unphysical constraint it would cause a phase transition to spin antiferromagnetism. No numerical calculation based on a conventional Hamiltonian finds a resonating valence bond state^{62–65}.

Experimental Constraints

As materials and experimental techniques improved over time, the purely empirical case for a new quantum state incompatible with the theory of metals became progressively weaker. After several years of failure Josephson tunneling was finally observed between YBa₂C₃O_{7– δ} and Pb, thus dispelling concerns that cuprate superconductivity might not be a traditional Cooper pair condensate^{66,67}. Ideas about the non-fermionic nature of the superconductor’s excitation spectrum were laid to rest by observation sharp fermionic quasiparticles in photoemission⁶⁸. Controversy over the symmetry of the superconducting order parameter was settled in favor of *d*-wave pairing by observation of the node in photoemission, a sign change in Josephson tunneling, and half-integral trapped flux in magnetometry^{69–73}. Ideas about the non-existence of a Fermi surface were disproved by photoemission observation of Fermi surfaces in overdoped samples agreeing in detail with band structure and the Luttinger sum rule^{74,75}. And, finally, superconductors placed in magnetic fields strong enough to crush their superconductivity were found to exhibit quantum oscillations, thus demonstrating the presence of a Fermi surface at low-energy scales in the zero-temperature normal state^{76–78}.

The finite-temperature properties of the cuprates continued to be problematic, especially above the superconducting transition temperature near optimal doping⁷⁹. However, as the temperatures were lowered to zero the behavior inevitably evolved into something simple and conventional, most notably when the superconductivity was suppressed with a magnetic field⁸⁰. Repeated and consistent failure of the strange metal behavior to persist to low temperature has now demonstrated that it has nothing to do with quantum states of matter but is rather a critical phenomenon associated with a zero-temperature phase transition beneath the superconducting dome^{81–84}. The possibility that this phase transition is pseudogap development remains controversial^{85,86}.

The occurrence of the pseudogap below optimal doping is associated with the reconstruction of the Fermi surface into pockets, as would be expected if a density wave had formed⁸⁷. The pseudogap, first discovered in magnetic resonance and optical conductivity, was later identified in photoemission as a *d*-wave quasiparticle dispersion that persisted above the superconducting transition temperature^{88,89}. Subsequent experiments revealed

the existence of two d -wave gaps, one associated with the superconductivity and another antagonistic to it^{90–93}. Scanning tunneling microscopy has now shown that pseudogap has complex position-dependent structure that is inherently glassy^{94,95}. It has also shown that conventional fermionic quasiparticles exist in the presence of the pseudogap and that they have the ability to propagate coherently large distances through it and interfere⁹⁶.

Orbital Antiferromagnetism

Several years before the quantum oscillation discovery, a group of us predicted that a reconstructed Fermi surface would appear when the superconductivity was destroyed by a strong magnetic field¹². We argued that conventional translational symmetry breaking had to be the cause of the pseudogap because nothing else could be written down as actual equations. We proposed specifically that the pseudogap was the signature of orbital antiferromagnetism. Our grounds were (1) that there was no other way to account for a d -wave pseudogap that was compatible with the adiabatic principle and (2) that instability to such order was an unavoidable consequence of antiferromagnetic exchange stabilization of d -wave superconductivity out of a metallic parent. We named this order d -density wave (DDW) to distinguish it from the gauge theory flux vacua, which were mathematically similar but conceptually different^{97,98}. However, after much searching the predicted magnetic Bragg peaks were not found, so the purely empirical case for the order could not be made⁹⁹.

The subsequent discovery of quantum oscillations changed this situation. The original theoretical grounds for anticipating Fermi surface reconstruction had not changed, and attempts to reconcile it with the underlying quantum mechanics without doubling the unit cell proved impossible¹⁰⁰. The only explanation compatible with the adiabatic principle is that DDW order is, in fact, present in the cuprates, and that failure to detect clean magnetic Bragg peaks from it has been a consequence of pseudogap glassiness.

There is nothing extraordinary about orbital magnetism from the point of view of quantum mechanics. The 3P_2 ground state of the neutral O atom has a total magnetic moment of $3\mu_B$, $2\mu_B$ of which comes from the spin and $1\mu_B$ of which comes from the orbit. Orbital antiferromagnetism is normally quenched in solids, but is it conceptually no different from spin antiferromagnetism¹⁰¹.

The failure to find signature magnetic Bragg peaks contributed materially to the development of the Varma current-loop theory, which has many similar features but does not break translation symmetry^{102,103}. There is now some experimental support for this theory, although it is controversial^{104–109}. However, the loop current insulating state has the same problem the Mott insulator does: It cannot be written down in electron coordinates.

Both kinds of spontaneous current would be difficult to detect in conventional Cu or O magnetic resonance in any cuprate because of symmetry¹¹⁰.

II. ADIABATIC EVOLUTION

Let us now briefly review the idea of adiabatic evolution. We imagine a fictitious Hamiltonian \mathcal{H}_0 , usually noninteracting electrons moving in a periodic potential, that is easy to diagonalize. We then add a “perturbation” $\lambda(\mathcal{H} - \mathcal{H}_0)$, where \mathcal{H} is the true Hamiltonian, and slowly increase λ from 0 to 1. Each time we infinitesimally increment λ , one of two things happens: either (1) the ground state and low-lying excitations remain in one-to-one correspondence, or (2) they do not. If the former is the case, we say that the system has remained in the same quantum phase. If the latter is the case, we say that it has undergone a quantum phase transition^{111,112}.

Adiabatic mapping is what enables universal characterization of low-energy excitations inside a given phase. Thus, for example, when we say that electrons in a conventional metal behave as though they do not interact, we really mean that there is an adiabatic path back to \mathcal{H}_0 that does not encounter any phase transitions. Were there no such path, it would make no sense to talk about a metal’s electrons and holes as abstractions, or to write down equations for them that involve only small effective interactions. The electrons in a conventional metal interact extremely strongly, as do electrons in solids generally. The correct Hamiltonian is always

$$\begin{aligned} \mathcal{H} = & - \sum_j \frac{\hbar^2}{2m} \nabla_j^2 - \sum_\alpha \frac{\hbar^2}{2M_\alpha} \nabla_\alpha^2 - \sum_{j\alpha} \frac{Z_\alpha e^2}{|\mathbf{r}_j - \mathbf{R}_\alpha|} \\ & + \sum_{j < k} \frac{e^2}{|\mathbf{r}_j - \mathbf{r}_k|} + \sum_{\alpha < \beta} \frac{Z_\alpha Z_\beta}{|\mathbf{R}_\alpha - \mathbf{R}_\beta|} \end{aligned} \quad (1)$$

where \mathbf{r}_j denotes the location of the j th electron and \mathbf{R}_α denotes the location of an ion of mass M_α . The kinetic and potential energies of the valence electrons are therefore always comparable by virtue of the virial theorem. It is not true that the Coulomb interactions in the cuprates are enormously bigger than they are in other solids, such as elemental Si or Na metal. They are just the same.

Whether the interactions of Eq. (1) are strong enough to destabilize the metallic state necessarily and always is an interesting question, but an academic one in light of the enormous body of experimental precedent in metals^{113,114}. Moreover the idea that metals might be inherently unstable at low-energy scales does not in any way invalidate computational procedures based on adiabatic evolution from a fictitious noninteracting parent state, which is to say, sums of conventional metallic Feynman graphs¹¹⁵.

It is not necessary that phase transitions should occur at isolated points in the interval $0 < \lambda < 1$, but this is

usually the case. The reason is renormalization¹¹⁶. As a system is made larger and larger its measured properties eventually begin to change in a deterministic way. A renormalization fixed point is a Hamiltonian whose low-energy excitation spectrum stays the same when the system size is made larger. If all the perturbations to this Hamiltonian diminish under renormalization, we say the fixed point is attractive, and we associate it with a stable state of matter. If at least one perturbation grows with renormalization, we say the fixed point is repulsive, and we associate it with a continuous phase transition. The difference between repulsion and attraction is why phases of matter occupy open sets of λ values, while the transitions between them tend to occur at points.

The logical inconsistency of the Mott insulator concept is now easy to spot: It is perfectly reasonable that a system should pass through a new phase of matter on the way from $\lambda = 0$ (a metal) to $\lambda = 1$ (a d -wave superconductor) but one is obligated to say what it is.

III. FUNDAMENTAL EQUATIONS

Correct equations for the cuprate problem are easy to write down once one accepts that they must describe adiabatic evolution out of the density functional band structure. The latter is described adequately by²⁵

$$\begin{aligned} \mathcal{H}_0 = & -t \sum_{\langle jk \rangle} \sum_{\sigma} (c_{j\sigma}^{\dagger} c_{k\sigma} + c_{k\sigma}^{\dagger} c_{j\sigma}) \\ & + t' \sum_{\langle j\ell \rangle} \sum_{\sigma} (c_{j\sigma}^{\dagger} c_{\ell\sigma} + c_{\ell\sigma}^{\dagger} c_{j\sigma}) \end{aligned} \quad (2)$$

where $\langle jk \rangle$ denotes the set of near-neighbor pairs of N sites on a planar square lattice of lattice constant b and $\langle j\ell \rangle$ denotes the set of second-neighbor pairs. This description is inaccurate far from the fermi surface, but the high-energy excitations poorly described are not important.

Fermi Liquid Parameters

Each time one increments λ the small perturbations renormalize to an effective Hamiltonian of the form

$$\begin{aligned} \Delta\mathcal{H} = & U \sum_j c_{j\uparrow}^{\dagger} c_{j\downarrow}^{\dagger} c_{j\downarrow} c_{j\uparrow} \\ & + \frac{J}{2} \sum_{\langle jk \rangle} \sum_{\sigma\sigma'} \left[c_{j\sigma}^{\dagger} c_{k\sigma'}^{\dagger} c_{k\sigma} c_{j\sigma'} - \frac{1}{2} c_{j\sigma}^{\dagger} c_{k\sigma'}^{\dagger} c_{k\sigma'} c_{j\sigma} \right] \\ & + V_t \sum_{\langle jk \rangle} \sum_{\sigma\sigma'} (c_{j\sigma}^{\dagger} c_{k\sigma} + c_{k\sigma}^{\dagger} c_{j\sigma}) (c_{j\sigma'}^{\dagger} c_{j\sigma'} + c_{k\sigma'}^{\dagger} c_{k\sigma'} - \frac{1}{2}) \end{aligned}$$

$$\begin{aligned} & + V_n \sum_{\langle jk \rangle} \sum_{\sigma\sigma'}^{2N} c_{j\sigma}^{\dagger} c_{k\sigma'}^{\dagger} c_{k\sigma'} c_{j\sigma} \\ & + V_c \sum_{\langle jk \rangle}^{2N} \left[c_{j\uparrow}^{\dagger} c_{j\downarrow}^{\dagger} c_{k\downarrow} c_{k\uparrow} + c_{k\uparrow}^{\dagger} c_{k\downarrow}^{\dagger} c_{j\downarrow} c_{j\uparrow} \right] \end{aligned} \quad (3)$$

This represents the most general set of fermi liquid parameters allowed by symmetry. Only pairwise interactions are relevant because the perturbation excites a quantum-mechanical gas of quasiparticles that is dilute. Only lattice terms closer than second neighbors are relevant because these exhaust the low angular momentum scattering channels. All terms associated with bonds must be rotationally invariant about the bond axis and reflection symmetric. All terms must be spin-rotationally invariant and time-reversal symmetric. The parameters can, in principle, be energy-dependent, as they are, for example, if they are mediated by phonons, but this is irrelevant at the lowest energy scales. The difference between phonon-mediated pairing and purely electronic pairing is retardation, and this shows up only in high-energy spectroscopy¹¹⁵. The parameters can also be doping dependent, but I find that they are not.

All the various parts of \mathcal{H} added by incrementing λ renormalize into fermi liquid parameters by definition if the system has not yet made a phase transition out of the metallic state¹¹⁷⁻¹²⁰. But they also do if a phase transition has occurred along the way that is mild. This is why conventional superconductors may be described simply with Feynman graph sums¹¹⁵. The new state is still a quantum-mechanical combination of electron and holes of the parent metal.

Since $\mathcal{H} + \Delta\mathcal{H}$ is the most general effective Hamiltonian possible, *all* of the behaviors of the cuprate superconductors must be contained in it. There is no other possibility.

Band Rigidity

We may immediately set V_t to zero. Were it present its main effect would be to renormalize the kinetic energy in the doping-dependent way

$$t \rightarrow t + V_t \sum_{\sigma} \left[\langle c_{j\sigma}^{\dagger} c_{j\sigma} \rangle + \langle c_{k\sigma}^{\dagger} c_{k\sigma} \rangle - \frac{1}{2} \right] \quad (4)$$

where $\langle \rangle$ denotes ground state expectation value. However, angle-resolved photoemission measurements find the asymptotic nodal fermi velocity to be $\hbar v_F = 2.0$ eV \AA for both p -type and n -type materials, regardless of doping¹²¹⁻¹²³.

The absence of such a term makes sense physically. Doping dependence of t simply means that the potential

barrier through which the electrons tunnel depends on electron density. Such dependence is already taken care of in the band structure through self-consistency.

The observed Fermi velocity requires $t = 0.19$ eV, which is about half the value predicted by the native band structure²⁵. The value of $t' = 0.1t$ is also fixed by photoemission, although it is also consistent with calculations¹²⁴.

IV. HARTREE-FOCK SOLUTION

The ground state $|\Psi\rangle$ is characterized by the expectation values

$$\begin{aligned} \langle c_{j\sigma}^\dagger c_{k\sigma} \rangle &= \chi_R \pm i\chi_I & \langle c_{j\sigma}^\dagger c_{l\sigma} \rangle &= \chi'_R \\ \langle c_{j\uparrow}^\dagger c_{k\downarrow}^\dagger \rangle &= \xi & \langle c_{j\sigma}^\dagger c_{j\sigma} \rangle &= \frac{n}{2} \pm (-1)^\sigma s \end{aligned} \quad (5)$$

with the signs as in Fig. 1. The order parameter ξ describes d -wave superconductivity (DWS). The order parameter χ_I describes orbital antiferromagnetism (DDW). The order parameter s describes spin antiferromagnetism (SDW). χ_R and χ'_R are not order parameters but measures of the ground state kinetic energy. n is the site occupancy.

To simplify the calculation we constrain both χ_I and s to be periodic in the doubled unit cell. This creates a mild artifact of allowing the system to conduct electricity at all nonzero dopings. If this constraint is relaxed, SDW domain walls form, trapping carriers and causing the system to insulate everywhere SDW order is developed^{125–129}. The similar problem with DDW, while important, is less severe because (1) the DDW quasiparticle spectrum is gapless at half-filling and (2) the DDW symmetry breaking is discrete.

The Hartree-Fock approximation is expressed either as a sum of rainbow Feynman graphs or as a single Slater determinant variational ground state¹⁰. In either case, each electron effectively moves in an average field generated by all the others. The variational ground state $|\Psi\rangle$ takes the form

$$|\Psi\rangle = \prod_{\mathbf{q}\nu} (u_{\mathbf{q}\nu} + v_{\mathbf{q}\nu} c_{\mathbf{q}\nu\uparrow}^\dagger c_{-\mathbf{q}\nu\downarrow}^\dagger) |0\rangle \quad (6)$$

where

$$c_{\mathbf{q}\nu\sigma}^\dagger = \sqrt{\frac{2}{N}} \sum_j (a_{j\sigma}^{\mathbf{q}\nu})^* \exp(i\mathbf{q} \cdot \mathbf{r}_j) c_{j\sigma}^\dagger \quad (7)$$

is the creation operator for an electron of crystal momentum \mathbf{q} and spin σ in band ν . The index ν is required because both kinds of antiferromagnetism double the unit cell. As usual, the vector \mathbf{r}_j denotes the location of the

j th site. The coefficients $a_{j\sigma}^{\mathbf{q}\nu}$ are the same in every unit cell and satisfy

$$\begin{bmatrix} \tilde{\Delta} & \tilde{\epsilon}_{\mathbf{q}} + i\tilde{\Delta}_{\mathbf{q}} \\ \tilde{\epsilon}_{\mathbf{q}} - i\tilde{\Delta}_{\mathbf{q}} & -\tilde{\Delta} \end{bmatrix} \begin{bmatrix} a_{1\uparrow}^{\mathbf{q}\pm} \\ a_{2\uparrow}^{\mathbf{q}\pm} \end{bmatrix} = \pm \tilde{E}_{\mathbf{q}} \begin{bmatrix} a_{1\uparrow}^{\mathbf{q}\pm} \\ a_{2\uparrow}^{\mathbf{q}\pm} \end{bmatrix} \quad (8)$$

$$\begin{bmatrix} -\tilde{\Delta} & \tilde{\epsilon}_{\mathbf{q}} + i\tilde{\Delta}_{\mathbf{q}} \\ \tilde{\epsilon}_{\mathbf{q}} - i\tilde{\Delta}_{\mathbf{q}} & \tilde{\Delta} \end{bmatrix} \begin{bmatrix} a_{1\downarrow}^{\mathbf{q}\pm} \\ a_{2\downarrow}^{\mathbf{q}\pm} \end{bmatrix} = \pm \tilde{E}_{\mathbf{q}} \begin{bmatrix} a_{1\downarrow}^{\mathbf{q}\pm} \\ a_{2\downarrow}^{\mathbf{q}\pm} \end{bmatrix} \quad (9)$$

where

$$\tilde{\epsilon}_{\mathbf{q}} = - \left[t + \left(\frac{3}{4}J + V_n - V_c \right) \chi_R \right] \left[\cos(q_x) + \cos(q_y) \right] \quad (10)$$

$$\tilde{t} = t + \left(\frac{3}{4}J + V_n - V_c \right) \chi_R \quad (11)$$

$$\tilde{\Delta}_{\mathbf{q}} = \left(\frac{3}{4}J + V_n + V_c \right) \chi_I \left[\cos(q_x) - \cos(q_y) \right] \quad (12)$$

$$\tilde{\Delta} = (U + 2J)s \quad (13)$$

$$\tilde{E}_{\mathbf{q}} = \sqrt{\tilde{\epsilon}_{\mathbf{q}}^2 + \tilde{\Delta}^2 + \tilde{\Delta}_{\mathbf{q}}^2} \quad (14)$$

in units for which the bond length b equals 1.

The absence of band mixing in Eq. (6) is a consequence of the system's special symmetries. Combining Eq. (8) with the complex conjugate of Eq. (9) in the presence of d -wave superconductivity, we obtain the Nambu matrix

$$\mathcal{H}_{\mathbf{q}} = \begin{bmatrix} \tilde{\Delta} - \tilde{\mu} & \tilde{\epsilon}_{\mathbf{q}} + i\tilde{\Delta}_{\mathbf{q}} & 0 & \tilde{\theta}_{\mathbf{q}}^* \\ \tilde{\epsilon}_{\mathbf{q}} - i\tilde{\Delta}_{\mathbf{q}} & -\tilde{\Delta} - \tilde{\mu} & \tilde{\theta}_{\mathbf{q}}^* & 0 \\ 0 & \tilde{\theta}_{\mathbf{q}} & \tilde{\mu} + \tilde{\Delta} & -\tilde{\epsilon}_{\mathbf{q}} + i\tilde{\Delta}_{\mathbf{q}} \\ \tilde{\theta}_{\mathbf{q}} & 0 & -\tilde{\epsilon}_{\mathbf{q}} - i\tilde{\Delta}_{\mathbf{q}} & \tilde{\mu} - \tilde{\Delta} \end{bmatrix} \quad (15)$$

where

$$\tilde{\theta}_{\mathbf{q}} = \left(\frac{3}{4}J - V_n \right) \xi \left[\cos(q_x) - \cos(q_y) \right] \quad (16)$$

$$\tilde{\mu}_{\mathbf{q}} = \mu - 2t' \left[\cos(q_x + q_y) + \cos(q_x - q_y) \right] \quad (17)$$

with μ as the chemical potential. However since

$$\begin{bmatrix} 1 & 0 & 0 & 0 \\ 0 & 1 & 0 & 0 \\ 0 & 0 & 0 & 1 \\ 0 & 0 & 1 & 0 \end{bmatrix} \mathcal{H}_{\mathbf{q}} \begin{bmatrix} 1 & 0 & 0 & 0 \\ 0 & 1 & 0 & 0 \\ 0 & 0 & 0 & 1 \\ 0 & 0 & 1 & 0 \end{bmatrix}$$

$$= \begin{bmatrix} \tilde{\Delta} - \tilde{\mu}_{\mathbf{q}} & \tilde{\epsilon}_{\mathbf{q}} + i\tilde{\Delta}_{\mathbf{q}} & \tilde{\theta}_{\mathbf{q}}^* & 0 \\ \tilde{\epsilon}_{\mathbf{q}} - i\tilde{\Delta}_{\mathbf{q}} & -\tilde{\Delta} - \tilde{\mu}_{\mathbf{q}} & 0 & \tilde{\theta}_{\mathbf{q}}^* \\ \tilde{\theta}_{\mathbf{q}} & 0 & \tilde{\mu}_{\mathbf{q}} - \tilde{\Delta} & -\tilde{\epsilon}_{\mathbf{q}} - i\tilde{\Delta}_{\mathbf{q}} \\ 0 & \tilde{\theta}_{\mathbf{q}} & -\tilde{\epsilon}_{\mathbf{q}} + i\tilde{\Delta}_{\mathbf{q}} & \tilde{\mu}_{\mathbf{q}} + \tilde{\Delta} \end{bmatrix} \quad (18)$$

the eigenvalues of $\mathcal{H}_{\mathbf{q}}$ are $\pm E_{\mathbf{q}}^{\pm}$, where

$$E_{\mathbf{q}}^{\pm} = \sqrt{(\pm\tilde{E}_{\mathbf{q}} - \tilde{\mu}_{\mathbf{q}})^2 + |\tilde{\theta}_{\mathbf{q}}|^2} \quad (19)$$

The bands therefore do not mix, and we have

$$u_{\mathbf{q}\pm} = \sqrt{\frac{E_{\mathbf{q}}^{\pm} + (\pm\tilde{E}_{\mathbf{q}} - \tilde{\mu}_{\mathbf{q}})}{2E_{\mathbf{q}}^{\pm}}} \quad (20)$$

$$v_{\mathbf{q}\pm} = \sqrt{\frac{E_{\mathbf{q}}^{\pm} - (\pm\tilde{E}_{\mathbf{q}} - \tilde{\mu}_{\mathbf{q}})}{2E_{\mathbf{q}}^{\pm}}} \quad (21)$$

Quasiparticle Energies

The operators

$$b_{\mathbf{q}\nu\uparrow} = u_{\mathbf{q}\nu} c_{\mathbf{q}\nu\uparrow} + v_{\mathbf{q}\nu} c_{\mathbf{q}\nu\downarrow}^{\dagger} \quad (22)$$

$$b_{\mathbf{q}\nu\downarrow} = u_{\mathbf{q}\nu} c_{\mathbf{q}\nu\downarrow} - v_{\mathbf{q}\nu} c_{\mathbf{q}\nu\uparrow}^{\dagger} \quad (23)$$

destroy $|\Psi\rangle$. Their adjoints create quasiparticles of energy $E_{\mathbf{q}}^{\nu}$.

Pairwise Contractions

With a variational ground state of the form of Eq. (6), the expected interaction energy is the sum of all pairwise contractions. Thus, for example, the second term of Eq. (3) gives a ground state expectation value of

$$\begin{aligned} & \sum_{\sigma\sigma'} \langle \Psi | c_{j\sigma}^{\dagger} c_{k\sigma'}^{\dagger} c_{k\sigma} c_{j\sigma'} - \frac{1}{2} c_{j\sigma}^{\dagger} c_{k\sigma'}^{\dagger} c_{k\sigma'} c_{j\sigma} | \Psi \rangle \\ &= -\frac{3}{2} \left\{ \langle c_{j\uparrow}^{\dagger} c_{k\downarrow}^{\dagger} \rangle \langle c_{k\downarrow} c_{j\uparrow} \rangle + \langle c_{j\downarrow}^{\dagger} c_{k\uparrow}^{\dagger} \rangle \langle c_{k\uparrow} c_{j\downarrow} \rangle \right\} \\ & - \sum_{\sigma\sigma'} (1 - \frac{1}{2} \delta_{\sigma\sigma'}) \langle c_{j\sigma}^{\dagger} c_{k\sigma} \rangle \langle c_{k\sigma'}^{\dagger} c_{j\sigma'} \rangle \\ & + \sum_{\sigma\sigma'} (\delta_{\sigma\sigma'} - \frac{1}{2}) \langle c_{j\sigma}^{\dagger} c_{j\sigma} \rangle \langle c_{k\sigma'}^{\dagger} c_{k\sigma'} \rangle \end{aligned}$$

$$= -3|\xi|^2 - 3(\chi_R + i\chi_I)(\chi_R - i\chi_I) - 2s^2 \quad (24)$$

Thus this term stabilizes all three kinds of order. Here we have used the relations

$$\langle c_{j\uparrow}^{\dagger} c_{k\downarrow}^{\dagger} \rangle = \langle c_{k\uparrow}^{\dagger} c_{j\downarrow}^{\dagger} \rangle = \langle c_{k\downarrow} c_{j\uparrow} \rangle^* = \langle c_{j\downarrow} c_{k\uparrow} \rangle^* \quad (25)$$

$$\langle c_{j\uparrow}^{\dagger} c_{k\uparrow} \rangle = \langle c_{j\downarrow}^{\dagger} c_{k\downarrow} \rangle = \langle c_{k\uparrow}^{\dagger} c_{j\uparrow} \rangle^* = \langle c_{k\downarrow}^{\dagger} c_{j\downarrow} \rangle^* \quad (26)$$

implicit in Eq. (6).

The last term in Eq. (3) gives

$$\begin{aligned} & \langle \Psi | c_{j\uparrow}^{\dagger} c_{j\downarrow}^{\dagger} c_{k\downarrow} c_{k\uparrow} + c_{k\uparrow}^{\dagger} c_{k\downarrow}^{\dagger} c_{j\downarrow} c_{j\uparrow} | \Psi \rangle \\ &= \langle c_{j\uparrow}^{\dagger} c_{k\uparrow} \rangle \langle c_{j\downarrow}^{\dagger} c_{k\downarrow} \rangle + \langle c_{k\uparrow}^{\dagger} c_{j\uparrow} \rangle \langle c_{k\downarrow}^{\dagger} c_{j\downarrow} \rangle \\ &= (\chi_R + i\chi_I)^2 + (\chi_R - i\chi_I)^2 \quad (27) \end{aligned}$$

It thus has no effect on either DWS or SDW but stabilizes DDW.

The remaining two ‘‘coulombic’’ terms in Eq. (3) give

$$\begin{aligned} & \sum_{\sigma\sigma'} \langle \Psi | c_{j\sigma}^{\dagger} c_{k\sigma'}^{\dagger} c_{k\sigma'} c_{j\sigma} | \Psi \rangle \\ &= 2|\xi|^2 - 2(\chi_R + i\chi_I)(\chi_R - i\chi_I) + n^2 \quad (28) \end{aligned}$$

per Eq. (24) and

$$\begin{aligned} & \langle \Psi | c_{j\uparrow}^{\dagger} c_{j\downarrow}^{\dagger} c_{j\downarrow} c_{j\uparrow} | \Psi \rangle = \langle c_{j\uparrow}^{\dagger} c_{j\uparrow} \rangle \langle c_{j\downarrow}^{\dagger} c_{j\downarrow} \rangle \\ &= \left(\frac{n}{2}\right)^2 - s^2 \quad (29) \end{aligned}$$

Variational Energy

Thus the total expected ground state energy is

$$\begin{aligned} & \frac{1}{N} \frac{\langle \Psi | \mathcal{H}_0 + \Delta\mathcal{H} | \Psi \rangle}{\langle \Psi | \Psi \rangle} = -8t\chi_R + 8t'\chi'_R \\ & + \left[\frac{n^2}{4} - s^2\right] U + \left[2n^2 + 4|\xi|^2 - 4\chi_R^2 - 4\chi_I^2\right] V_n \\ & - \left[3\chi_R^2 + 3\chi_I^2 + 3|\xi|^2 + 2s^2\right] J + \left[4\chi_R^2 - 4\chi_I^2\right] V_c \quad (30) \end{aligned}$$

Self-Consistency Equations

The extremal condition

$$\delta \left\{ \frac{\langle \Psi | \mathcal{H}_0 + \Delta \mathcal{H} | \Psi \rangle}{\langle \Psi | \Psi \rangle} \right\} = 0 \quad (31)$$

then gives the equations

$$n = \frac{1}{8\pi^2} \sum_{\pm} \int_{-\pi}^{\pi} \int_{-\pi}^{\pi} \left[1 - \frac{(\pm \tilde{E}_{\mathbf{q}} - \tilde{\mu}_{\mathbf{q}})}{E_{\mathbf{q}}^{\pm}} \right] dq_x dq_y \quad (32)$$

$$s = -\frac{1}{(U+2J)s} \times \frac{1}{16\pi^2} \sum_{\pm} \int_{-\pi}^{\pi} \int_{-\pi}^{\pi} \frac{\tilde{\Delta}_{\mathbf{q}}^2}{\pm \tilde{E}_{\mathbf{q}}} \left[1 - \frac{(\pm \tilde{E}_{\mathbf{q}} - \tilde{\mu}_{\mathbf{q}})}{E_{\mathbf{q}}^{\pm}} \right] dq_x dq_y \quad (33)$$

$$\chi_R = -\frac{1}{t} \times \left(\frac{1}{64\pi^2} \right) \sum_{\pm} \int_{-\pi}^{\pi} \int_{-\pi}^{\pi} \frac{\tilde{\epsilon}_{\mathbf{q}}^2}{\pm \tilde{E}_{\mathbf{q}}} \left[1 - \frac{(\pm \tilde{E}_{\mathbf{q}} - \tilde{\mu}_{\mathbf{q}})}{E_{\mathbf{q}}^{\pm}} \right] dq_x dq_y \quad (34)$$

$$\chi_I = -\frac{1}{(3J/4 + V_n + V_c)\chi_I} \times \left(\frac{1}{64\pi^2} \right) \sum_{\pm} \int_{-\pi}^{\pi} \int_{-\pi}^{\pi} \frac{\tilde{\Delta}_{\mathbf{q}}^2}{\pm \tilde{E}_{\mathbf{q}}} \left[1 - \frac{(\pm \tilde{E}_{\mathbf{q}} - \tilde{\mu}_{\mathbf{q}})}{E_{\mathbf{q}}^{\pm}} \right] dq_x dq_y \quad (35)$$

$$\xi = \frac{1}{(3J/4 - V_n)\xi} \times \left(\frac{1}{64\pi^2} \right) \sum_{\pm} \int_{-\pi}^{\pi} \int_{-\pi}^{\pi} \frac{\tilde{\theta}_{\mathbf{q}}^2}{E_{\mathbf{q}}^{\pm}} dq_x dq_y \quad (36)$$

Iterating these to convergence locates the minimum variational ground state energy

V. LIMITING CASES

As a preliminary to fitting the parameters U , J , V_c and V_n to experiment we shall consider a handful of limiting cases.

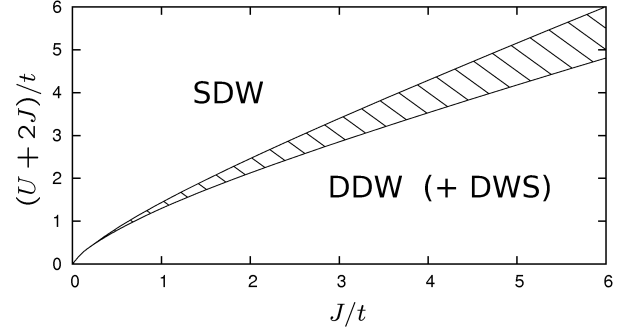


FIG. 2: Phase diagram for the particle-hole symmetric ($t' = 0$) case at half filling ($n = 1$) given by Eqs. (32) - (36) with all parameters except t , U , and J set to zero and with superconductivity suppressed by artificially holding ξ to zero. The quantum phase transition between SDW and DDW is second order with a small region of coexistence (hashed). DDW is exactly degenerate with DWS at half-filling when only U and J are nonzero. This is a consequence of a special symmetry described in Appendix A.

Half-Filling Antiferromagnetism

Let us first set all the parameters except t , J , and U to zero and adjust the chemical potential μ to half-filling ($n = 1$). The superconductivity is problematic in this limit, so let us also force $\xi = 0$ by hand. Iterating Eqs. (32) - (36) to self-consistency, we obtain the result shown in Fig. 2. There are two second-order phase transitions bounding a region of coexistence between spin antiferromagnetism (spin density wave SDW) and orbital antiferromagnetism (d -density wave DDW).

It is immediately clear from this figure that pure exchange characterized by J tends to stabilize SDW and DDW equally. For $J > 0.2t$ one needs $U < 0$, which is unphysical, to achieve coexistence. But the more important observation is that the requisite U is relatively small. The boundary in question is also actually multicritical. DDW and DWS are exactly degenerate in this limit. This may be seen by comparing Eqs. (35) and (36), but the actual cause is a special symmetry described in Appendix A.

This result thus shows that strongly correlated superexchange ($J = 4t^2/U \ll U$) cannot account quantitatively for DWS in the cuprates¹³⁰. One of the key experimental features of these materials is that small amounts of doping, a delicate perturbation, can violently disrupt the SDW and completely replace it with DWS. This implies that the system lies near a phase boundary. But Fig. 2 shows that the purely magnetic system cannot be near the phase boundary between SDW and DWS unless U is small. This observation is backed up by the large body of numerical work on the Hubbard model, which shows that it does not account well for properties of the cuprates¹³¹.

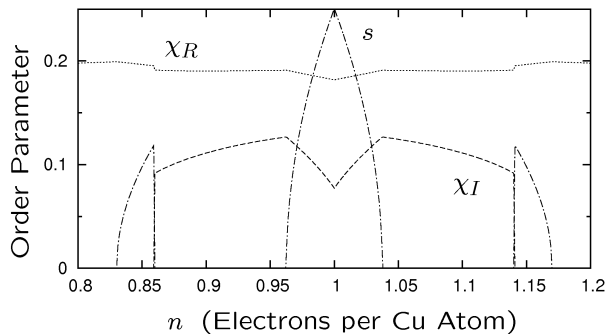


FIG. 3: Order parameters s and χ_I defined by Eqs. (5) as a function of n obtained by solving Eqs. (32) - (36) with ξ artificially held to zero for the case of $U+2J = 5.7t$, $J = 5.9t$, and $t' = V_c = V_n = 0$. The kinetic energy parameter χ_R is also plotted. The parameters are determined by the conditions (1) $s = 0.25$ at $n = 1$ and (2) the system lie near the upper edge of the coexistence curve of Fig. 2. The occurrence of phase transitions at 4% and 14% and 16% doping is a general and robust consequence of these two constraints. The re-entrance at 14% is first order.

SDW vs. DDW

Let us next relax the condition that $n = 1$ and repeat the calculation of Fig. 2, again artificially forcing $\xi = 0$, with fixed values of $U + 2J = 5.7t$ and $J = 5.9t$. These parameters are unphysically large, in part because $\tilde{t}/t \simeq 1.8$, per Eq. (11). They are fit to the conditions that (1) the system lie near the upper edge of the coexistence region in Fig. 2 and (2) the spin moment at half-filling be $s = 0.25$, half the maximum classically allowed value. A moment of this size is characteristic of the insulating cuprates¹³²⁻¹³⁵. The result, shown in Fig. 3, reveals that the SDW is destroyed by a doping of 4%, a number characteristic of spin antiferromagnetism disappearance of the cuprates. SDW is supplanted at this density by DDW, a pseudogap candidate with a d -wave quasiparticle spectrum. DDW itself then becomes unstable at 14% doping, exactly where the optimal superconducting T_c is observed in the cuprates and where the pseudogap is observed to disappear. There is a slight first-order re-entrance of SDW at 14% when the DDW vanishes, indicating an intense struggle for dominance between the two kinds of order. Neither the specific transition doping densities nor the order parameter functional forms are fit.

Why this sequence of phase transitions takes place is easy to understand physically. Figure 4 shows the evolution of density of states

$$\mathcal{D}(E) = \frac{1}{8\pi^2} \sum_{\pm} \int_{-\pi}^{\pi} \int_{-\pi}^{\pi} \delta(E \pm \tilde{E}_{\mathbf{q}}) dq_x dq_y \quad (37)$$

as doping is increased. The rough equivalence of the two orders at half-filling, reflected in equality of their energy

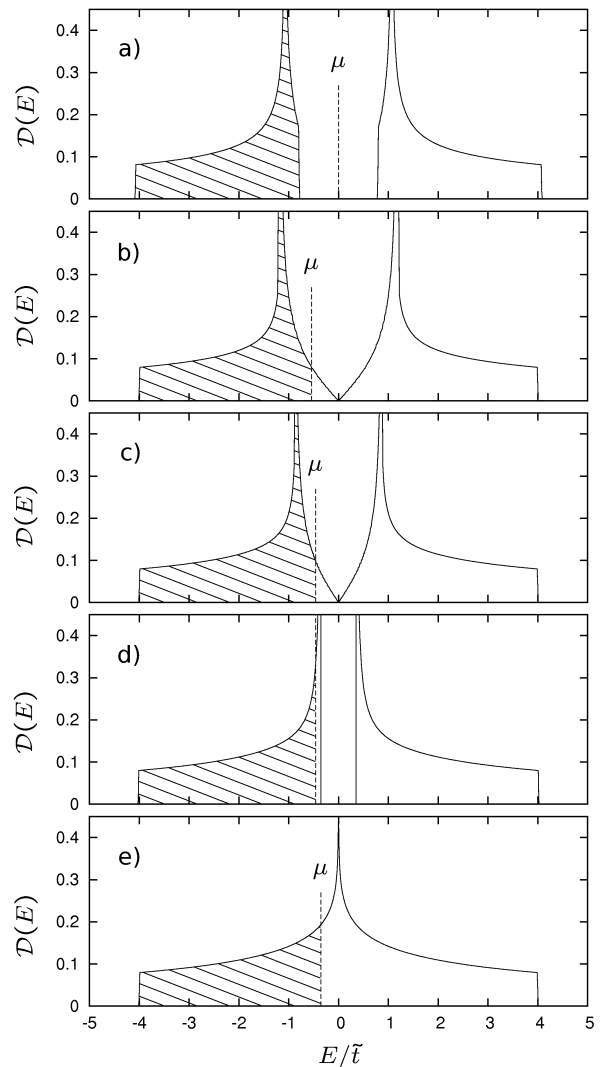


FIG. 4: Density of states $\mathcal{D}(E)$ defined by Eq. (37) for the calculation of Fig. 3 at the doping densities (a) $n = 1.000$, (b) $n = 0.962$, (c) $n = 0.860$, (d) $n = 0.859$, and (e) $n = 0.831$. The energy unit is \tilde{t} defined by Eq. (11). The shaded region is occupied. The chemical potential μ is the same in (c) and (d), as required at a first-order transition.

gaps, becomes unbalanced in favor of DDW when carriers are added because DDW, which has a node, allows them to be added at zero energy. Deeper doping then destabilizes DDW because it causes the Fermi surface to contract around the lines $q_x = \pm q_y$, where the state's node prevents it from extracting condensation energy. SDW order, which can extract condensation energy from this region, is then briefly resurrected, but it shortly falls victim to the Fermi surface shrinkage that occurs as doping is increased further.

The larger implication of Fig. 3 is that *any* system with a moment of $s = 0.25$ and rough balance between SDW and DDW at half filling will have phase transitions when doped at densities consistent with those observed

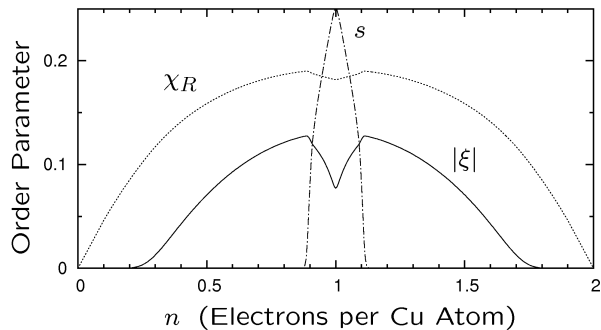


FIG. 5: Order parameters s and ξ defined by Eqs. (5) as a function of n obtained by solving Eqs. (32) - (36) for the case of $U + 2J = 5.7t$, $J = 5.9t$, and $t' = V_c = V_n = 0$. This is the same calculation as that in Fig. 3 but with the $\xi = 0$ constraint relaxed. The $n = 1$ value of $|\xi|$ exactly equals the $n = 1$ value of χ_I in Fig. 3, as required by the symmetry described in Appendix A.

in the cuprates.

SDW vs. DWS

Let us now repeat the calculation of Fig. 3 with the $\xi = 0$ constraint removed. The result, shown in Fig. 5, reveals that DWS now overwhelms DDW completely. The effect may be understood as an analog of a spin flop¹³⁶. The two kinds of order are exactly degenerate at $n = 1$, the way the x , y and z components of an ideal antiferromagnet are, as described in Appendix A. But the nesting condition required to stabilize DDW becomes degraded at any finite doping while DWS, which does not require nesting, remains robust. Adding carriers is thus analogous to adding an anisotropy field to the antiferromagnet, and the system responds by “flopping” to DWS.

The persistence of SDW to 12% doping in Fig. 5 also shows that DWS is less effective at crushing the SDW at low dopings than DDW is, even though it is more stable. The reason is that DWS does not exploit any special degeneracies of the band nesting and thus does not use them up and make them unavailable to SDW formation the way DDW would. Reentrant spin antiferromagnetism is also absent in Fig. 5, but this is a simple consequence of the persistence of nonzero ξ to high dopings.

The coexistence of DWS with SDW everywhere the latter is developed in Fig. 5 is allowed by the special (imposed) symmetries of the problem, which guarantee that spin antiferromagnetism fights superconductivity through gap formation only, not through pair breaking. The system can then become superconducting by exciting electrons across the SDW gap quantum mechanically and binding them into Cooper pairs there. A system nominally an insulator in this way becomes a superconductor. The effect is shown more explicitly in Fig. 6, where the superconducting spectral function

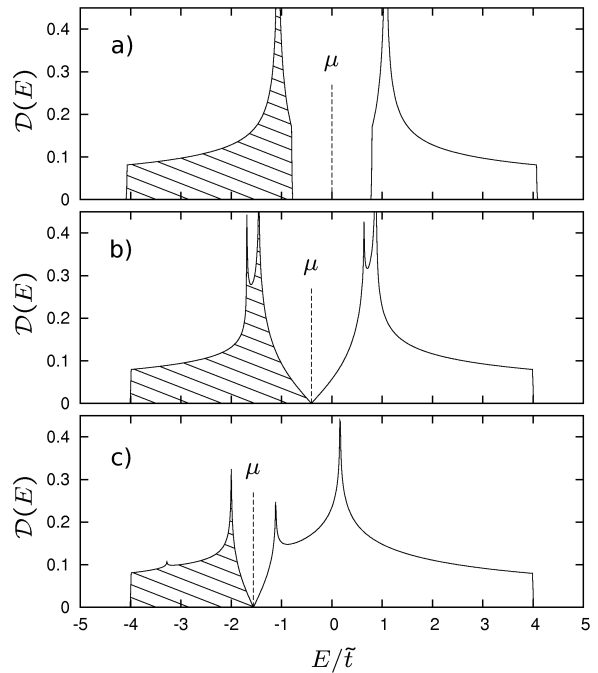


FIG. 6: Spectral function $\mathcal{D}(E)$ defined by Eq. (38) for the calculation of Fig. 5 at doping densities (a) $n=0.1$, (b) $n = 0.865$, and (c) $n = 0.5$. The system is superconducting in all three cases. The energy unit is \tilde{t} defined by Eq. (11). The shaded region is hole-like (i.e. the signal measured in photoemission).

$$\mathcal{D}(E) = \frac{1}{16\pi^2} \sum_{\pm} \times \int_{-\pi}^{\pi} \int_{-\pi}^{\pi} \left\{ \left[1 - \frac{(\pm \tilde{E}_{\mathbf{q}} - \tilde{\mu}_{\mathbf{q}})}{E_{\mathbf{q}}^{\pm}} \right] \delta(E - \tilde{\mu}_{\mathbf{q}} + E_{\mathbf{q}}^{\pm}) + \left[1 + \frac{(\pm \tilde{E}_{\mathbf{q}} - \tilde{\mu}_{\mathbf{q}})}{E_{\mathbf{q}}^{\pm}} \right] \delta(E - \tilde{\mu}_{\mathbf{q}} - E_{\mathbf{q}}^{\pm}) \right\} dq_x dq_y \quad (38)$$

is plotted. As doping increases the SDW gap eventually collapses, restoring the d -wave node.

DWS vs. DDW

Let us now get all three order parameters to appear in the phase diagram by repeating the calculation of Fig. 5 in the presence of $V_c > 0$. This parameter breaks the degeneracy between DDW and DWS at half filling, encouraging the former over the latter. The result is shown in Fig. 7. In order to maintain the half-filling conditions implicit in Figs. 3 and 5, we accompany the increase of V_c with an adjustment of the parameters U and J that

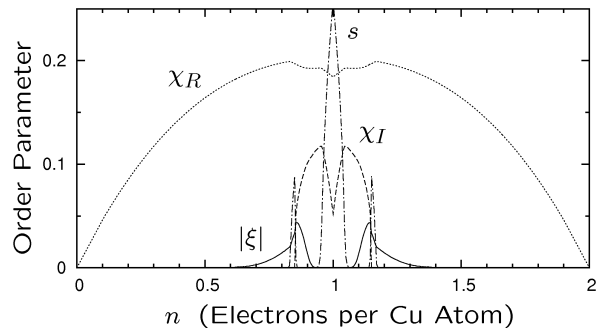


FIG. 7: Order parameters s , χ_I and ξ defined by Eqs. (5) as a function of n obtained by solving Eqs. (32) - (36) for the case of $U + 2J = 2.5t$, $V_c = 1.3t$, $J = 0.7t$, and $t' = V_n = V_t = 0$. The parameters $(U + 2J)/\tilde{t}$ and $(3J/4 + V_n + V_c)/\tilde{t}$, with \tilde{t} defined as in Eq. (11), are about the same as those assumed in Figs. 3 and 5. The reentrant spin antiferromagnetism at 15% doping is the same as that seen in Fig. 3.

keeps $(U + 2J)/\tilde{t}$ and $(3J/4 + V_n + V_c)/\tilde{t}$ constant, per Eqs. (11) and (33) - (35). When V_c is increased to the value used in Fig. 7, this causes the interaction parameters U , J and V_c all to become reasonably sized (i.e. comparable to t), and, even more importantly, causes U to switch from negative to positive. The behavior of Fig. 3 is now restored, this time legitimately, but DDW is accompanied by doping-dependent DWS, with which it coexists. The latter first acquires significant magnitude when the SDW is destroyed at 5% and then rises up as the DDW dies away, peaking at 15% where the latter disappears, and then declining rapidly. The sequence of events is identical to that observed in p -type cuprates.

The result of Fig. 7 cannot be achieved using $V_n > 0$. The half-filling degeneracy of DDW and DWS is broken the same way by both parameters, but $V_n > 0$ has the effect of suppressing DWS, per Eq. (36). This suppression can be counteracted by increasing the value of J , but this then requires making U more negative, per Eq. (33). Negative U is highly unphysical. Were it present, it would stabilize s -wave superconductivity, a phenomenon not observed in the cuprates.

Particle-Hole Asymmetry

Let us now introduce particle-hole asymmetry by repeating the calculation of Fig. 7 with an added $t' = 0.1t$. The result is shown in Fig. 8. The pseudogap is now completely absent on the n -type side, and the re-entrant spin antiferromagnetism has disappeared from both sides.

The ability of such a small change in the underlying band structure to violently rearrange the phase diagram is consistent with the variability of cuprate experiments, both among different materials and among samples of the same material prepared different ways. It occurs because small perturbations tip the fine balance among order-

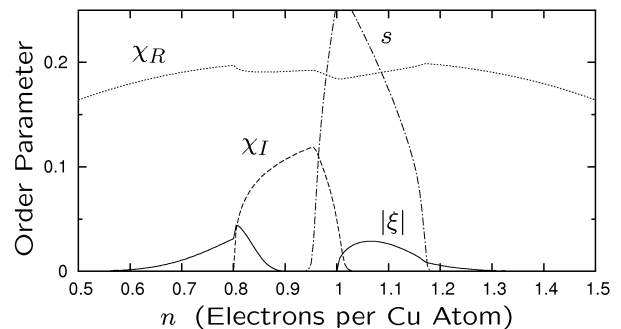


FIG. 8: The same calculation as in Fig. 7 except with band asymmetry $t' = 0.1t$. The remaining parameters are $U + 2J = 2.5t$, $V_c = 1.3t$, $J = 0.7t$, and $V_n = V_t = 0$. The large region of coexistence between DWS and SDW on the n -type side is an artifact of having constrained the SDW to be periodic in the doubled unit cell. When this condition is relaxed, the system insulates due to domain wall trapping everywhere SDW order is developed¹²⁵⁻¹²⁹

ings. Defects and crystal boundaries would be expected to rearrange the order parameters locally in a similar fashion, thus causing large effects that have no analog in semiconductors. This result is also consistent with the observed complexity of lattice instabilities in these materials¹³⁵. Describing the latter requires addition of an electron-phonon interaction to $\mathcal{H}_0 + \Delta\mathcal{H}$, but doing so is straightforward given that the only effect of moving atoms around is to change the underlying band structure.

VI. PARAMETRIC CONSTRAINTS

Figures 7 and 8 show that the interaction parameters J , U , and V_c are fixed by the magnitudes of s , χ_I , and ξ , and that $V_n = 0$ is fixed by the overall shape of the phase diagram. The conclusion that $V_n = 0$ resolves the important controversy of whether antiferromagnetic exchange or near-neighbor attraction, possibly phonon-mediated, causes high- T_c superconductivity. Only the former is both physically reasonable and compatible with experiment.

The reason that one cannot have $V_n < 0$ is subtle and requires some discussion. Only $J > 0$ and $V_n < 0$ have the ability to stabilize d -wave superconductivity, so at least one of them must be present and sizable. However, a $J > 0$ of the requisite magnitude is already present, as demonstrated by the antiferromagnetism of the undoped insulator. Adding $V_n < 0$ would further stabilize d -wave superconductivity, but unfortunately it would do so near half-filling and destabilize the pseudogap. To restore the pseudogap, one would then have to compensate by making either J or V_c more positive, per Eq. (35). But, J actually has to *decrease* if the superconducting aspects of Fig. 7 are to remain the same, per Eq. (36). The required increase in V_c would then severely narrow the

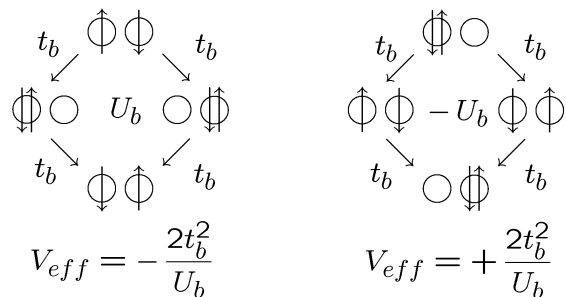


FIG. 9: Illustration of the generation of V_c and J together through superexchange as described by Eq. (40). Cuprate antiferromagnetism is caused by blocking.¹³⁰ The bond quantum mechanics thus deforms adiabatically to a Hubbard model characterized by parameters t_b and U_b . Second-order perturbation theory then gives an effective matrix element V_{eff} for exchanging a pair of electrons that is negative because the intermediate states have positive energy. The matrix element for Cooper pair tunneling has the opposite sign because the intermediate states have negative energy.

quasiparticle bandwidth, per Eq. (11), an effect not observed experimentally. Accordingly, V_n can be neither negative nor positive but must be zero.

The conclusion that $V_n = 0$ also makes sense physically. The parameter V_n is a Coulomb interaction. There is fundamentally no reason for it to be negative, just as there is no reason for U to be negative. Indeed one's first guess would be that both parameters had been mostly accounted for in the generation of the band structure. A parameter $V_n < 0$ would also tend to stabilize s -wave superconductivity unless prevented from doing so by a sufficiently large U . The latter would have to be large enough to prevent mixed $d+s$ superconductivity, a phenomenon not observed in any part of the cuprate phase diagram. The parameter $J > 0$ by contrast is not only demonstrably present but something unique to the cuprates.

In addition to properly balancing the phase diagram, the parameter $V_c > 0$ has three important effects that indicate it is not only useful but actually physically necessary: (1) it enables U to be positive, (2) it reduces J to a reasonable size, and (3) it enables \tilde{t} to be less than t . The latter is particularly important. The parameter \tilde{t} fixes physical quasiparticle bandwidth, a quantity observed experimentally not to be broadened, but it also sets quasiparticle Fermi velocity. Were $\tilde{t}/t > 1$, the oscillator strength of the Fermi sea conductivity pole would exceed the total f -sum rule, which is fixed by t solely, thus indicating that the system was not in its ground state. This sum rule problem is discussed further Section VII in the context of the superfluid density.

Given the insight that postulating $J > 0$ makes no sense without also postulating $V_c > 0$ of roughly the same magnitude, the source of the latter is easily identified: It is a secondary aspect of superexchange. This is illustrated in Fig. 9. Spin antiferromagnetism is due to

blocking¹³⁰. One knows this because the spin-orbit and magnetic dipole interactions in typical antiferromagnets are too small to account for the observed spin stiffness. The bond quantum mechanics may therefore be adiabatically deformed to a Hubbard model characterized by parameters t_b and U_b . In terms of the four configurational states

$$\begin{aligned}
 |1\rangle &= c_{j\uparrow}^\dagger c_{j\downarrow}^\dagger |0\rangle & |2\rangle &= c_{k\uparrow}^\dagger c_{k\downarrow}^\dagger |0\rangle \\
 |3\rangle &= c_{j\uparrow}^\dagger c_{k\downarrow}^\dagger |0\rangle & |4\rangle &= c_{k\uparrow}^\dagger c_{j\downarrow}^\dagger |0\rangle
 \end{aligned}
 \tag{39}$$

we then have the Hamiltonian

$$\mathcal{H}_{bond} = \begin{bmatrix} U_b & 0 & t_b & t_b \\ 0 & U_b & t_b & t_b \\ t_b & t_b & 0 & 0 \\ t_b & t_b & 0 & 0 \end{bmatrix}
 \tag{40}$$

Second-order perturbation theory then gives a spin-exchange matrix element of $-2t_b^2/U_b$ and a Cooper pair tunneling matrix element of $+2t_b^2/U_b$.

Correlation corrections to the properties of metals are notoriously difficult to calculate from first principles, especially if they are performed by summing Feynman graphs. In graphical sums, the negative-energy denominators required to obtain $V_c > 0$ show up in the reverse time orderings¹⁰. Such calculations are beyond the scope of this work. The purpose of Eq. (40) is only to show that it is physically reasonable for $V_c > 0$ to appear whenever $J > 0$ does.

The parameter fits used in generating Figs. 7 and 8 thus lead to the conclusion that superexchange mediated by the bonding oxygen atom, not Coulomb repulsion on the copper sites, is responsible for all three ordering phenomena.

VII. SUPERCONDUCTING PROPERTIES

In what follows we shall assume the parameters used to generate Fig. 1: $U = 0.76t$, $J = 0.75t$, $V_c = 0.87t$, $t' = 0.1t$, $V_n = V_t = 0$, and $t = 0.19$ eV. These amount to a small fine-tuning of the parameters of Fig. 8.

Energy Gap

Figure 10 compares the maximum gaps computed using Eq. (32) - (36) with pseudogap and superconducting gap value estimated by Hühner *et al* from a variety of experimental sources¹³⁷. The latter include scanning tunneling microscopy, photoemission, Raman scattering, break junction tunneling, magnetic resonance, inelastic neutron scattering, thermal transport and Andreev scattering¹³⁸⁻¹⁴⁷. The experimental plot is qualitatively

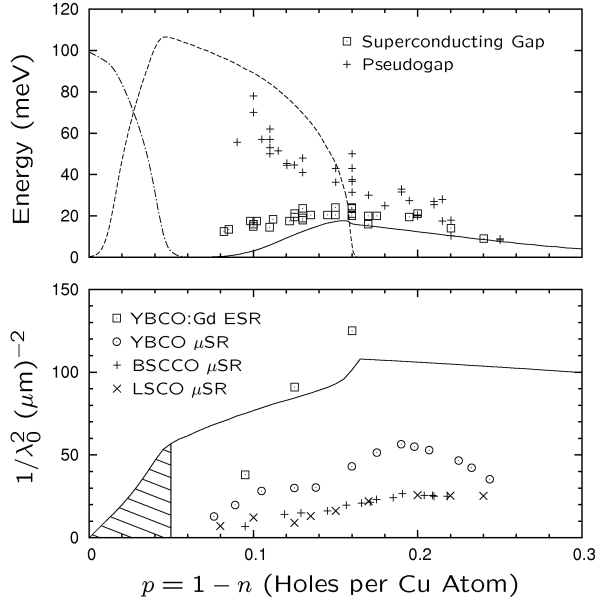


FIG. 10: Top: Comparison of SDW gap $(U + 2J)s$ (dash-dotted line), maximum DDW gap $(3J + 4V_c)\chi_I$ (dashed line) and maximum superconducting gap $3J|\xi|$ (solid line) computed using Eqs. (32) - (36) with values of the pseudogap (+) and superconducting gaps (\square) inferred from a variety of experiments by H \ddot{u} fn \ddot{u} r *et al.*¹³⁷. Bottom: London penetration depth calculated with Eq. (41) compared with μ SR measurements on polycrystalline samples reported by Tallon *et al* (+, \times , \circ) and in-plane ESR measurements on oxygen-ordered YBCO:Gd samples by Pereg-Barnea *et al.*¹⁴⁹⁻¹⁵¹. About half the disparity in the YBCO results are attributable to penetration depth anisotropy, which causes the powder average of $1/\lambda_0^2$ to be about 2/3 of the in-plane one. The hatching indicates insulation due to SDW domain-wall trapping. The oscillator strength in this region does not reside at zero frequency but instead at a low, but finite, frequency characteristic of the trapping^{154,155}. The calculations assume the parameters of Fig. 1: $U = 0.76t$, $J = 0.75t$, $V_c = 0.87t$, $t' = 0.1t$, $V_n = V_t = 0$, and $t = 0.19$ eV.

similar to that of Le Tacon *et al.* and of Valenzuela and Bascones but is in absolute units^{90,92}. The assignment of specific values to the experimental gaps is somewhat subjective because they are not sharply defined. A reasonable estimate of the error bar is 30%. Particularly important are the Andreev reflection experiments, which show that particle-hole mixing characteristic of superconducting order vanishes at an energy scale much lower than that of the pseudogap^{147,148}.

Figure 10 severely constrains the choice of U , J , and V_c . The scale of superconducting gap fixes $J = 0.75t$. The scale of the pseudogap fixes $3J/4 + V_c = 1.43t$. The condition that $s \simeq 0.25$ at half filling fixes $U + 2J = 2.26t$. These parameters then place the system at the edge of the half-filling coexistence region of Fig. 2 (with the substitution $J \rightarrow J + 4V_c/3$ keeping $U + 2J$ fixed), thus causing the two phase transitions take place at their

experimentally observed doping values of 5% and 16%.

London Penetration Depth

The zero-temperature London penetration depth λ_0 is given by

$$\frac{1}{\lambda_0^2} = \frac{4\pi e^2}{\hbar^2 c^2} \left(\frac{t}{a}\right) \tilde{n}_s = 151 (\mu\text{m})^{-2} \tilde{n}_s \quad (41)$$

where $a = 5.84 \text{ \AA}$ is an interlayer spacing appropriate for YBCO and \tilde{n}_s in the effective superfluid density per Cu atom

$$\tilde{n}_s = \frac{1}{16\pi^2 t} \sum_{\pm}$$

$$\int_{-\pi}^{\pi} \int_{-\pi}^{\pi} \left[1 - \frac{(\pm \tilde{E}_{\mathbf{q}} - \tilde{\mu})}{E_{\mathbf{q}}^{\pm}} \right] \nabla_{\mathbf{q}}^2 (\pm \tilde{E}_{\mathbf{q}} - \tilde{\mu}) \quad (42)$$

The superfluid density is not a well-defined quantity, so the choice of t as the conversion factor between $1/\lambda_0^2$ and \tilde{n}_s is somewhat arbitrary. It corresponds to the effective mass formula

$$\frac{1}{\lambda_0^2} = \frac{4\pi e^2}{m^* c^2} \left(\frac{\tilde{n}_s}{ab^2}\right) \quad m^* = \frac{\hbar^2}{tb^2} = 2.50 m_e \quad (43)$$

with a bond length $b = 4 \text{ \AA}$.

The formal justification of Eq. (42) when DDW order is developed is complicated by the fact that the DDW order parameter χ_I is gauge-variant, while the Hamiltonian parameter J that gives rise to it is not. Handling this properly requires executing a vertex correction, which is technically beyond the scope of this work. However, it is easy to see on physical grounds that Eq. (42) must be correct. It says that each quasiparticle carries electric charge e and moves with a speed that is the momentum derivative of its energy, just as occurs in SDW. The quasiparticles of DDW and SDW must behave similarly because orbital antiferromagnetism and spin antiferromagnetism are aptly analogous.

Figure 11 shows the superfluid density \tilde{n}_s calculated using Eq. (42) and the parameters of Fig. 1 as a function of doping. It is free-electron-like except when the DDW and SDW orders develop near $n \rightarrow 1$, when it is strongly suppressed. This reflects the reorganization of the Fermi surface into pockets. Loss of superfluid density due to an elementary Fermi surface reconstruction is fully consistent with the finding of Tallon *et al.* that the ratio of the superconducting temperature T_c and the specific heat jump remains constant in this limit while both quantities individually vanish¹⁴⁹.

The values of $1/\lambda_0^2$ implicit in Fig. 11 through Eq. (41) are compared with experiment in Fig. 10¹⁴⁹⁻¹⁵¹.

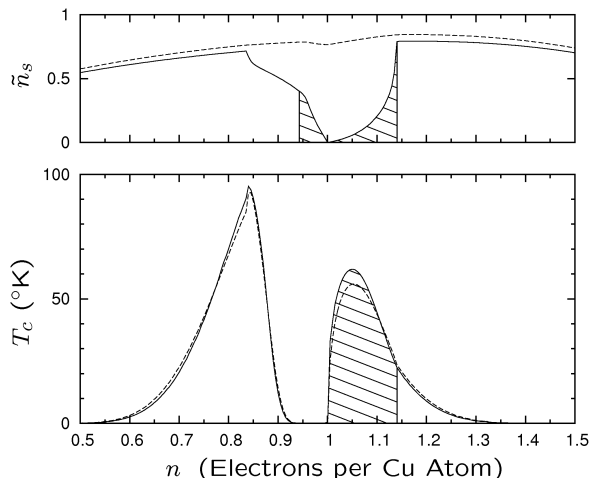


FIG. 11: Top: Superfluid density \tilde{n}_s defined by Eq. (42). The dashed curve is the total f-sum rule given by Eq. (44). Bottom: Superconducting transition temperature defined by Eq. (46). The dashed curve is the maximum superconducting gap divided by 2.2, i.e. $3J|\xi|/2.2k_B$. The hatching has the same meaning as in Fig. 10: This region is insulating, rather than superconducting, because of carrier trapping at SDW domain walls. The computations assume the parameters of Fig. 1: $U = 0.76t$, $J = 0.75t$, $V_c = 0.87t$, $t' = 0.1t$, $V_n = V_t = 0$, and $t = 0.19$ eV.

The large variability among them is symptomatic of disorder degradation. The proper comparison to make is thus with the best samples at optimal doping. The good agreement in these cases confirms $\tilde{n}_s \simeq 1$.

The nonzero superfluid density for $0.95 < n < 1.14$ in Fig. 11 ($0 < p < 0.05$ in Fig. 10) is an artifact of having forced the SDW to periodic in the doubled unit cell. Relaxing this condition will cause the quasiparticles to trap in domain walls, thus forcing the superfluid density to zero, in agreement with experiment^{125–129}. The system is an insulator over the entire range in which SDW is developed—with the possible exception of $n \simeq 1.4$, where coexistence of SDW and DWS has been reported^{152,153}. The superfluid oscillator strength in question, however, is not lost but is simply transported upward to a small, but finite frequency characteristic of the trapping. This is seen experimentally in the lightly-doped cuprates as mid-infrared absorption^{154,155}. It is centered at about 0.6 eV in $\text{La}_{2-x}\text{Sr}_x\text{CuO}_4$.

Figure 11 also shows that the total f-sum rule

$$\tilde{n}_{total} = 4\chi_R - 8\left(\frac{t'}{t}\right)\chi'_R$$

derived in Appendix C, where

$$\chi'_R = \frac{1}{64\pi^2 t'} \sum_{\pm} \int_{-\pi}^{\pi} \int_{-\pi}^{\pi} \left[1 - \frac{(\pm \tilde{E}_{\mathbf{q}} - \tilde{\mu})}{E_{\mathbf{q}}^{\pm}} \right] (\mu - \tilde{\mu}) dq_x dq_y \quad (44)$$

per Eqs. (5), exceeds \tilde{n}_s . This is an important stability test. \tilde{n}_{total} is the sum of \tilde{n}_s plus all the additional optical oscillator strength at higher frequencies. If one had $\tilde{n}_s > \tilde{n}_{total}$ at any doping value, it would imply that the system had negative oscillator strength (laser gain) at higher frequencies, and thus that it was not in its ground state. But Eqs. (32) - (36) show that $\tilde{n}_s < \tilde{n}_{total}$ is enforced by $(3J/4 - V_c) < 0$. Thus Fig. 11 also shows that the presence of a $V_c > 0$ is required for $J > 0$ to make sense physically. Moreover, the particular values of these parameters used to generate Fig. 11 give \tilde{n}_s comparable to \tilde{n}_{total} except where the fermi surface is reconstructed. This means that nearly all of the oscillator strength is exhausted by the fermi surface pole, as would be expected on physical grounds.

Transition Temperature T_c

The relative largeness of the superfluid density near optimal doping implies that the superconducting transition temperature is not determined by phase fluctuations¹⁵⁶. The phase decoherence temperature cannot be any lower than the Kosterlitz-Thouless temperature¹⁵⁷

$$k_B T_{KT} = \frac{\pi}{8} \frac{\hbar^2}{m^* b^2} \tilde{n}_s = \frac{\pi}{8} t \tilde{n}_s \quad (45)$$

which lies above 433 °K ($\tilde{n}_s = 0.5$) over the entire range of interest. It is thus too high to matter.

The transition temperature must therefore be determined by the weakening of the DWS order parameter by excitation of conventional BCS quasiparticles. It is computed by substituting $\xi = 0$ in Eqs. (32) - (36) and then replacing Eq. (36) with

$$1 = \left(\frac{3}{4}J\right) \frac{1}{16\pi^2} \sum_{\pm} \int_{-\pi}^{\pi} \int_{-\pi}^{\pi} \frac{1}{|\pm \tilde{E}_{\mathbf{q}} - \tilde{\mu}|} \times \tanh\left(\frac{E_{\mathbf{q}}^{\pm}}{2k_B T_c}\right) \left[\cos(q_x) - \cos(q_y)\right]^2 dq_x dq_y \quad (46)$$

One obtains the transition temperatures shown in Fig. 11. Also shown is the maximum $T = 0$ superconducting gap $4J|\xi|$ divided by $2.2k_B$. The factor of 2.2 is similar to the 2.37 reported by Tallon *et al.* for a slightly different model¹⁴⁹. A factor of approximately 2.5 was assumed by Hüfner *et al.* in inferring the data points plotted in Fig. 10¹³⁷.

VIII. OTHER PROPERTIES

Insulation

The SDW equations are well known to be unstable to antiferromagnetic domain wall formation whenever the

SDW gap is nonzero^{125–129}. This is consistent with the antiferromagnetic discommensuration observed by neutron scattering in doped insulating $\text{La}_{1.95}\text{Sr}_{0.05}\text{CuO}_4$ ¹⁵⁸. The mathematics of twisting is briefly reviewed in Appendix B. For the parameter range considered here, domain wall formation has no significant effect on the SDW gap magnitude but simply causes the added carriers to trap. This trapping occurs in two ways. The first is that domain walls already present preferentially bind added carriers the way impurities in a semiconductor do. The second is that added carriers create domain walls and self-trap in them if the system is annealed. Domain wall formation is inherently glassy and thus difficult to describe mathematically. It is also sensitive to details, such as sample preparation and the 5 meV anisotropy energy associated with preferential ordering of the spins in the x - y plane¹⁵⁹. The latter is due to spin-orbit coupling, which is left out of Eq. (3). As a consequence, there is presently no general agreement on what the true ground state of the doped antiferromagnet is.

The small region of coexistence between SDW and DWS in the range $1.12 < n < 1.15$ reported by Yu *et al.* and Luo *et al.* is consistent with Fig. 11^{152,153}. The SDW and DWS order parameters lie in different irreducible representations of the system's symmetry group. Provided that they are competing energetically and that a conventional Ginzburg-Landau description remains correct in the presence of disorder, the system must have either (1) a first-order transition between them or (2) two second-order transitions in and out of a coexistence region.

The trapping effects in the cuprates actually extend over the entire insulating range $0.95 < n < 1.14$. This must be so because insulation is physically impossible in a translationally-invariant system that can be continuously doped. The proof is very simple: Applying a nonuniform voltage is the same thing as changing the chemical potential locally. Thus the conventional metallic behavior in the range $0.95 < n < 1$ implicit in Fig. 11 is also an artifact.

Domain wall formation is also an issue with the DDW order, which is arguably the cause of the glassiness observed in scanning tunneling microscopy near optimal doping⁹⁶. However it is less serious in that case because (1) the DDW state has a node at which carriers may be added with minimal energy and (2) the DDW order parameter is Ising-like. The latter implies that continuous twisting is impossible, and thus that domain walls have a much higher energy cost than the domain walls of the SDW do.

Magnon Spectrum

The ladder approximation for the spin susceptibility is given by¹⁶⁰

$$\chi_{\mathbf{q}}(\omega) = \left\{ [\chi_{\mathbf{q}}^{(0)}(\omega)]^{-1} + U \begin{bmatrix} 1 & 0 \\ 0 & 1 \end{bmatrix} \right.$$

$$\left. - J[\cos(q_x) + \cos(q_y)] \begin{bmatrix} 1 & 0 \\ 0 & -1 \end{bmatrix} \right\}^{-1} \quad (47)$$

where

$$\begin{aligned} \chi_{\mathbf{q}}^{(0)}(\omega) &= \frac{1}{8\pi^2} \int_{-\pi}^{\pi} \int_{-\pi}^{\pi} \left\{ \frac{1}{2E_{\mathbf{k}+\mathbf{q}}E_{\mathbf{k}}} \right. \\ &\times \begin{bmatrix} E_{\mathbf{k}+\mathbf{q}}E_{\mathbf{k}} - \tilde{\epsilon}_{\mathbf{k}+\mathbf{q}}\tilde{\epsilon}_{\mathbf{k}} + \tilde{\Delta}^2 & \tilde{\Delta}(E_{\mathbf{k}+\mathbf{q}} + E_{\mathbf{k}}) \\ \tilde{\Delta}(E_{\mathbf{k}+\mathbf{q}} + E_{\mathbf{k}}) & E_{\mathbf{k}+\mathbf{q}}E_{\mathbf{k}} - \tilde{\epsilon}_{\mathbf{k}+\mathbf{q}}\tilde{\epsilon}_{\mathbf{k}} + \tilde{\Delta}^2 \end{bmatrix} \\ &\times \frac{1}{\hbar\omega - (E_{\mathbf{k}+\mathbf{q}} + E_{\mathbf{k}}) + i\eta} + \frac{1}{2E_{\mathbf{k}+\mathbf{q}}E_{\mathbf{k}}} \\ &\times \begin{bmatrix} E_{\mathbf{k}+\mathbf{q}}E_{\mathbf{k}} - \tilde{\epsilon}_{\mathbf{k}+\mathbf{q}}\tilde{\epsilon}_{\mathbf{k}} + \tilde{\Delta}^2 & -\tilde{\Delta}(E_{\mathbf{k}+\mathbf{q}} + E_{\mathbf{k}}) \\ -\tilde{\Delta}(E_{\mathbf{k}+\mathbf{q}} + E_{\mathbf{k}}) & E_{\mathbf{k}+\mathbf{q}}E_{\mathbf{k}} - \tilde{\epsilon}_{\mathbf{k}+\mathbf{q}}\tilde{\epsilon}_{\mathbf{k}} + \tilde{\Delta}^2 \end{bmatrix} \\ &\left. \times \frac{1}{-\hbar\omega - (E_{\mathbf{k}+\mathbf{q}} + E_{\mathbf{k}}) - i\eta} \right\} dq_x dq_y \quad (48) \end{aligned}$$

The ladder sum is formally similar to the random phase approximation in dielectric response, and is often referred to as the RPA for this reason even though the graphs in question are of the opposite sign. Including it is a standard method of computing spin fluctuation properties of SDW states¹⁶¹. Figure 12 shows how it effectively adds a large attractive interaction between the excited particle and hole, thereby binding them down out of the continuum to form a spin-1 magnon. The spin wave dispersion curve that results is compared in Fig. 12 with the inelastic neutron scattering measurements on La_2CuO_4 reported by Coldea *et al.*¹⁶². Although the RPA is notoriously inaccurate at short wavelengths, the disparity at the Brillouin zone edge in Fig. 12 is most likely not a computational problem but an SDW gap that is too small, particularly since this material has a larger magnetic moment than the other undoped cuprates¹³⁵. Raising U to $1.3t$, which increases s to 0.28, causes the computation to match experiment. The agreement at low-energy scales in either case is sufficient to demonstrate that the spin wave velocity is correctly computed.

Chemical Potential Jump

The chemical potential jump upon going from p type to n type is small^{163,164}. Exactly how small is not known exactly, for the experiments capable of measuring $\Delta\mu$ are difficult and plagued with the same interface chemistry sensitivity one finds in Schottky barrier heights. The calculation finds this jump to be twice the SDW gap at half filling, or 0.2 eV. Harima *et al.* originally reported a value of between 0.15 and 0.40 eV based core level shifts measured by x-ray photoemission¹⁶³. The core lines they

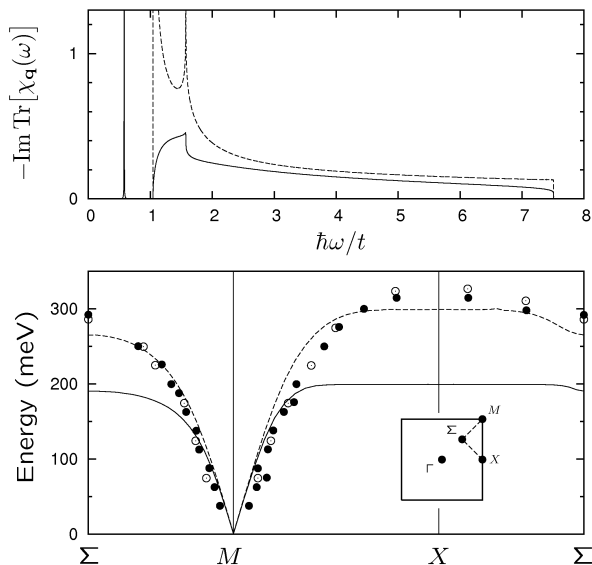


FIG. 12: Top: Imaginary part of the ladder sum (RPA) spin susceptibility defined by Eq. (47) for a momentum transfer of $(0.9\pi, 0.9\pi)$. The spin wave is the δ -function pole at $\hbar\omega = 0.58t$ bound down below the particle-hole continuum. The dashed curve is the bare susceptibility defined by Eq. (48). The computation assumes the parameters in Fig. 1: $U = 0.76t$, $J = 0.75t$, $V_c = 0.87t$, $t' = 0.1t$, $V_n = V_t = 0$, and $t = 0.19$ eV. Bottom: Comparison of magnon dispersion relation computed using Eqs. (47) and (48) with that measured by inelastic neutron scattering by Coldea *al.* for La_2CuO_4 ¹⁶². The spin wave velocity is $\hbar v_s = 1.0$ eV \AA . The open and solid symbols correspond to measurements taken at $T = 10$ K and $T = 295$ K. The dashed curve is a repeat of the calculation with $U = 1.3t$ and all other parameters the same. This raises the magnetic moment to $s = 0.28$. The inset shows the location of the symmetry points in the Brillouin zone.

reported were much broader than the shifts in question, and the core levels of different chemical species in the sample also shifted by different amounts, sometimes even in different directions. More recent experiments by Ikeda *et al.* on samples of $\text{Y}_{0.38}\text{La}_{0.62}\text{Ba}_{0.74}\text{La}_{0.26}\text{Cu}_3\text{O}_y$, which can be doped chemically in both directions, showed a larger jump of 0.8 eV¹⁶⁴. But both reported shifts are much smaller than the optical gap.

IX. SUMMARY AND CONCLUSION

The theory discussed in this paper differs substantially from most previous theoretical work on the cuprates in being based primarily on fundamental quantum mechanics, not empiricism. The underlying objective in constructing it is not to make a consistent mathematical phenomenology but to identify basic principles that can enable one to distinguish correct experiments from incorrect ones. This is especially important in a

field plagued with reproducibility and materials problems. While a handful of parameters discussed in this paper are fit to experiment, the equations themselves are not. A system evolved out of a fictitious metallic parent *must* have a low-energy excitation spectrum described by the Hamiltonian $\mathcal{H}_0 + \Delta\mathcal{H}$, defined by Eqs. (2) and (3), regardless of details. All important behaviors of the cuprates—antiferromagnetism, half-filling insulation, pseudogap and d -wave superconductivity—therefore *must* be contained in it. This is a different statement from suggesting yet another model for the cuprates.

A specific, and important, thing ruled out by $\mathcal{H}_0 + \Delta\mathcal{H}$ is Mott insulation. A system evolved adiabatically out of a metallic parent could very possibly undergo a quantum phase transition to a new state of matter that insulates, but one is obligated to write down equations for what this state is in terms of the low-lying excitations of the metal, ordinary electrons and holes, and make the case that the state is stable. A good example of such discipline is the Bardeen-Cooper-Schrieffer theory of superconductivity, which is a logical construct built on top of a metallic parent that is, in fact, fictional because it is absolutely unstable to superconductivity¹¹⁵. Thus, if the Mott insulator existed it would be possible to derive it starting from a Hamiltonian of the form of $\mathcal{H}_0 + \Delta\mathcal{H}$ with a specific choice of parameters. But this cannot be done. The Mott insulator therefore does not exist, and it cannot be used as a parent vacuum on which to build a theory of superconductivity. The Varma loop current insulator must be rejected for the same reason.

The Hamiltonian $\mathcal{H}_0 + \Delta\mathcal{H}$ requires the pseudogap to be bond current antiferromagnetism, or d -density wave (DDW). The reason is that DDW is fundamentally a crystal of d -wave Cooper pairs. It is automatically stabilized by any Hamiltonian that stabilizes d -wave superconductivity. Moreover, there is no latitude in the parameter space of $\mathcal{H}_0 + \Delta\mathcal{H}$ for stabilizing other states, particularly ones with the $d_{x^2-y^2}$ quasiparticle symmetry characteristic of the d -wave superconductor. DDW order *must* exist in the pseudogap regime of the cuprates, notwithstanding the problematic neutron searches for its signature magnetic Bragg peaks. The nuclear quadrupole resonance measurements reporting an absence of orbital current of any kind are therefore either misinterpreted or in error¹⁰⁹.

The number of free parameters in Eqs. (2) and (3) is actually three. The band parameters t and t' are fixed by band structure calculations and photoemission measurements on a wide variety of cuprates. The latter also require $V_t = 0$. Stabilizing the pseudogap near half filling requires $V_n = 0$. The three remaining parameters are fit to (1) the half filling antiferromagnetic moment, (2) the maximum pseudogap magnitude, and (3) the maximum superconducting T_c .

The parameter fit that results points unequivocally to the bonding O atom in the Cu-O plane as the pairing agent of high-temperature superconductivity. Superexchange mediated by this atom causes all three kinds of

order: spin antiferromagnetism (SDW), d -density wave (DDW), and d -wave superconductivity (DWS). Achieving proper balance among them requires that the atom also mediate repulsive Cooper pair tunneling, but this is fundamentally the same effect as antiferromagnetic spin exchange.

With the parameters fixed to values of Fig. 1, solution of the equations with conventional Hartree-Fock methods accounts quantitatively for the following aspects of cuprate superconductors:

1. A Fermi surface congruent with the underlying density functional band structure.
2. Spin antiferromagnetism (SDW) at half filling with a moment of about $s = 0.25$, or half the classical Ising value.
3. A spin wave velocity at half filling of $\hbar v_s \simeq 1.0$ eV Å.
4. Insulating behavior of the SDW for any value of doping.
5. Destruction of the SDW at 5% p -type doping.
6. Supplanting of the SDW at this doping by a pseudogap phase (DDW) characterized by a d -wave node.
7. The simultaneous reconstruction of the Fermi surface into pockets compatible with observed quantum oscillations.
8. A pseudogap magnitude of approximately 110 meV that decreases continuously to zero at 16% p -type doping.
9. An underlying quantum phase transition at 16% doping involving Fermi surface reconnection and thus massive carrier scattering.
10. The coexistence of the pseudogap (DDW) with d -wave superconductivity (DWS).
11. A d -wave superconducting gap maximizing at 20 meV at 16% doping and declining away from this optimal value.
12. A minimum in-plane London penetration depth of $\lambda_0 = 0.1 \mu\text{m}$ at optimal doping.
13. Strong suppression of the DWS superfluid density at p -type dopings less than optimal.
14. A superconducting transition temperature T_c maximizing at 93 K and equal at all important dopings to 1/2.2 times the maximum d -wave gap.
15. The absence of a pseudogap for n -type doping.
16. A direct transition from SDW to DDW at 15% n -type doping.

17. A chemical potential jump when going from p -type to n -type doping of approximately 0.2 eV.

The last of these items is sensitive to the half-filling magnetic moment and perhaps indicates an SDW gap that is too small. It is, however, consistent with experimental reports that the jump is much smaller than the optical gap.

The quality of these results, the extreme simplicity of the equations that produced them, and the reasonableness of the parameters required all argue strongly in favor of the theory's physical correctness.

Acknowledgments

I wish to thank S. Chakravarty for numerous insightful discussions about the cuprate problem over the years and for his determination in pursuing the empirical case for DDW. I also wish to thank S. Kivelson, T. Geballe, S.-C. Zhang, T. Devereaux and R. Martin for helpful discussions. Special thanks go to S. Raghu for calling the need for numerical work on this problem to my attention.

Appendix A: DDW/DWS Degeneracy

The equivalence of Eqs. (35) and (36) at half filling and $t' = 0$ results from a special symmetry familiar from studies of the Hubbard model¹⁶⁵. The Hamiltonian $\mathcal{H}_0 + \Delta\mathcal{H}$ defined by Eqs. (2) and (3) transforms simply under the unitary operator

$$\mathcal{U} = \prod_j^N \left[c_{j\downarrow}^\dagger - (-1)^j c_{j\downarrow} \right] \quad (\text{A1})$$

the action of which on the primary field operators is

$$\mathcal{U} c_{j\uparrow} \mathcal{U}^\dagger = c_{j\uparrow} \quad \mathcal{U} c_{j\downarrow} \mathcal{U}^\dagger = (-1)^j c_{j\downarrow} \quad (\text{A2})$$

Hubbard Parameter Transformations

The kinetic energy transforms to itself

$$\mathcal{U} (c_{j\uparrow}^\dagger c_{k\uparrow} + c_{j\downarrow}^\dagger c_{k\downarrow}) \mathcal{U}^\dagger = (c_{j\uparrow}^\dagger c_{k\uparrow} + c_{j\downarrow}^\dagger c_{k\downarrow}) \quad (\text{A3})$$

The on-site repulsion negates

$$\mathcal{U} \left[c_{j\uparrow}^\dagger c_{j\downarrow}^\dagger c_{j\downarrow} c_{j\uparrow} \right] \mathcal{U}^\dagger = -c_{j\uparrow}^\dagger c_{j\downarrow}^\dagger c_{j\downarrow} c_{j\uparrow} + c_{j\uparrow}^\dagger c_{j\uparrow} \quad (\text{A4})$$

The leftover $\sum_j c_{j\downarrow}^\dagger c_{j\downarrow}$ is a constant of the motion and may be dropped, which restores spin-rotational invariance.

Spin Exchange Transformation

The spin exchange term becomes

$$\begin{aligned} & \sum_{\sigma\sigma'} \mathcal{U} \left[c_{j\sigma}^\dagger c_{k\sigma'}^\dagger c_{k\sigma} c_{j\sigma'} - \frac{1}{2} c_{j\sigma}^\dagger c_{k\sigma'}^\dagger c_{k\sigma'} c_{j\sigma} \right] \mathcal{U}^\dagger \\ &= \frac{1}{2} \sum_{\sigma\sigma'} c_{j\sigma}^\dagger c_{k\sigma'}^\dagger c_{k\sigma'} c_{j\sigma} - \left[c_{j\uparrow}^\dagger c_{j\downarrow}^\dagger c_{k\downarrow} c_{k\uparrow} \right. \\ & \left. + c_{k\uparrow}^\dagger c_{k\downarrow}^\dagger c_{j\downarrow} c_{j\uparrow} \right] + \frac{1}{2} \left[1 - \sum_{\sigma} (c_{j\sigma}^\dagger c_{j\sigma} + c_{k\sigma}^\dagger c_{k\sigma}) \right] \end{aligned} \quad (\text{A5})$$

The last term in this expression is again a constant of the motion that may be dropped. Thus, in effect, the parameters J and $V_n - 2V_c$ turn into each other under the action of \mathcal{U} .

Remaining Transformations

The action of \mathcal{U} on V_n or V_c alone does not generate a spin invariant interaction. We have specifically

$$\begin{aligned} & \sum_{\sigma\sigma'} \mathcal{U} c_{j\sigma}^\dagger c_{k\sigma'}^\dagger c_{k\sigma'} c_{j\sigma} \mathcal{U}^\dagger \\ &= \sum_{\sigma\sigma'} (c_{j\uparrow}^\dagger c_{j\uparrow} - c_{j\downarrow}^\dagger c_{j\downarrow} + 1)(c_{k\uparrow}^\dagger c_{k\uparrow} - c_{k\downarrow}^\dagger c_{k\downarrow} + 1) \end{aligned} \quad (\text{A6})$$

Thus the combination $V_n - 2V_c$ is special.

Order Parameter Transformation

The DDW order parameter transforms under the action of \mathcal{U} to

$$\begin{aligned} & \mathcal{U} \left[\frac{1}{2i} \sum_{\sigma} (c_{j\sigma}^\dagger c_{k\sigma} - c_{k\sigma}^\dagger c_{j\sigma}) \right] \mathcal{U}^\dagger \\ &= \frac{1}{2i} \left[(c_{j\uparrow}^\dagger c_{k\uparrow} - c_{j\downarrow}^\dagger c_{k\downarrow}) - (c_{k\uparrow}^\dagger c_{j\uparrow} - c_{k\downarrow}^\dagger c_{j\downarrow}) \right] \quad (\text{A7}) \\ &= \frac{1}{2i} (\langle \Phi_j^\dagger | \sigma_z | \Phi_k \rangle - \langle \Phi_k^\dagger | \sigma_z | \Phi_j \rangle) \end{aligned}$$

where

$$\begin{aligned} |\Phi_j \rangle &= \begin{bmatrix} c_{j\uparrow} \\ c_{j\downarrow} \end{bmatrix} & \sigma_x &= \begin{bmatrix} 0 & 1 \\ 1 & 0 \end{bmatrix} \\ \sigma_y &= \begin{bmatrix} 0 & -i \\ i & 0 \end{bmatrix} & \sigma_z &= \begin{bmatrix} 1 & 0 \\ 0 & -1 \end{bmatrix} \end{aligned} \quad (\text{A8})$$

This is a bond spin current polarized in the z-direction. Thus, if $\mathcal{H}_0 + \Delta\mathcal{H}$ stabilizes DDW then $\mathcal{U}(\mathcal{H}_0 + \Delta\mathcal{H})\mathcal{U}^\dagger$ stabilizes bond spin current. But it must also stabilize spin currents in the x-direction and y-direction because it is spin-rotationally invariant. Back-transforming the latter we find

$$\begin{aligned} & \mathcal{U}^\dagger \left[\frac{1}{2i} (\langle \Phi_j^\dagger | \sigma_x | \Phi_k \rangle - \langle \Phi_k^\dagger | \sigma_x | \Phi_j \rangle) \right] \mathcal{U} \\ &= -\frac{(-1)^j}{2i} \left[(c_{k\uparrow}^\dagger c_{j\downarrow}^\dagger + c_{j\uparrow}^\dagger c_{k\downarrow}^\dagger) - (c_{k\downarrow} c_{j\uparrow} + c_{j\downarrow} c_{k\uparrow}) \right] \end{aligned} \quad (\text{A9})$$

$$\begin{aligned} & \mathcal{U}^\dagger \left[\frac{1}{2i} (\langle \Phi_j^\dagger | \sigma_y | \Phi_k \rangle - \langle \Phi_k^\dagger | \sigma_y | \Phi_j \rangle) \right] \mathcal{U} \\ &= (-1)^j \left[(c_{k\uparrow}^\dagger c_{j\downarrow}^\dagger + c_{j\uparrow}^\dagger c_{k\downarrow}^\dagger) + (c_{k\downarrow} c_{j\uparrow} + c_{j\downarrow} c_{k\uparrow}) \right] \end{aligned} \quad (\text{A10})$$

These represent the real and imaginary parts of the d -wave superconductor order parameter. Thus stabilizing DDW with U and J solely at half filling necessarily stabilizes DWS also.

Appendix B: Spiral States

The nature of SDW spirals is most easily illustrated by transforming to a basis in which each unit cell is the same. For simplicity we set all the parameters in $\mathcal{H} = \mathcal{H}_0 + \Delta\mathcal{H}$ to zero except for t , U and J . The unitary transformation

$$\mathcal{U}_{\mathbf{Q}} = \prod_j^N \exp \left\{ \frac{i}{2} (\mathbf{Q} \cdot \mathbf{r}_j) \left[c_{j\uparrow}^\dagger c_{j\downarrow} + c_{j\downarrow}^\dagger c_{j\uparrow} \right] \right\} \quad (\text{B1})$$

spirals the spin direction in the yz plane as one advances in the direction of \mathbf{Q} . Its actions on the elementary field operators are

$$\mathcal{U}_{\mathbf{Q}} c_{j\uparrow}^\dagger \mathcal{U}_{\mathbf{Q}}^\dagger = \cos\left(\frac{\mathbf{Q} \cdot \mathbf{r}_j}{2}\right) c_{j\uparrow}^\dagger + i \sin\left(\frac{\mathbf{Q} \cdot \mathbf{r}_j}{2}\right) c_{j\downarrow}^\dagger \quad (\text{B2})$$

$$\mathcal{U}_{\mathbf{Q}} c_{j\downarrow}^\dagger \mathcal{U}_{\mathbf{Q}}^\dagger = \cos\left(\frac{\mathbf{Q} \cdot \mathbf{r}_j}{2}\right) c_{j\downarrow}^\dagger + i \sin\left(\frac{\mathbf{Q} \cdot \mathbf{r}_j}{2}\right) c_{j\uparrow}^\dagger \quad (\text{B3})$$

The ansatz of a single-Slater-determinant ground state periodic in the twisted unit cell gives the Hartree-Fock Hamiltonian

$$\mathcal{H}_{\mathbf{q}}^{HF} = \epsilon_{\mathbf{q}}^{(0)} \begin{bmatrix} 1 & 0 \\ 0 & 1 \end{bmatrix} + \epsilon_{\mathbf{q}} \begin{bmatrix} 0 & 1 \\ 1 & 0 \end{bmatrix} + \Delta \begin{bmatrix} 1 & 0 \\ 0 & -1 \end{bmatrix} \quad (\text{B4})$$

where

$$\epsilon_q = 2t \left[\sin\left(\frac{Q_x}{2}\right) \sin(q_x) + \sin\left(\frac{Q_y}{2}\right) \sin(q_y) \right]$$

$$\epsilon_q^{(0)} = -2t \left[\cos\left(\frac{Q_x}{2}\right) \cos(q_x) + \cos\left(\frac{Q_y}{2}\right) \cos(q_y) \right]$$

The corresponding quasiparticle dispersion relation is $\epsilon_q^{(0)} \pm E_q$, where

$$E_q = \sqrt{\epsilon_q^2 + \Delta^2} \quad (\text{B5})$$

When Q_x and Q_y both equal π , this reduces to the doubled unit cell case worked out in Section IV. We are interested in Q_x and Q_y both near π , but not equal to it. The SDW band gap is then preserved, and the self-consistency equation for Δ becomes

$$\Delta = (U - J[\cos(Q_x) + \cos(Q_y)])s \quad (\text{B6})$$

where

$$s = \frac{1}{8\pi^2} \int_{-\pi}^{\pi} \int_{-\pi}^{\pi} \frac{\Delta}{E_q} dq_x dq_y \quad (\text{B7})$$

$$\chi_R = \frac{1}{32\pi^2 t} \int_{-\pi}^{\pi} \int_{-\pi}^{\pi} \frac{\epsilon_q^2}{E_q} \quad (\text{B8})$$

The total expected energy is

$$\begin{aligned} \frac{\langle \mathcal{H} \rangle}{N} &= -8\chi_R t + \left(\frac{1}{4} - s^2\right) U \\ &+ [\cos(Q_x) + \cos(Q_y)]s^2 J \end{aligned} \quad (\text{B9})$$

The effect of twisting on the corresponding density of states

$$\mathcal{D}(E) = \frac{1}{8\pi^2} \sum_{\pm} \int_{-\pi}^{\pi} \int_{-\pi}^{\pi} \delta(E - \epsilon_q^{(0)} \pm E_q) dq_x dq_y \quad (\text{B10})$$

is shown in Fig. 13. At a very small cost in variational energy, a spiral twist narrows the band gap, thus lowering the energy of added carriers. This implies that twisted antiferromagnetic domain walls trap carriers and cause insulation.

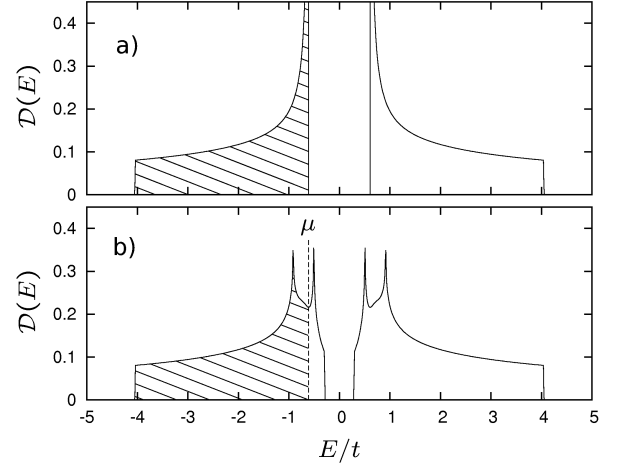


FIG. 13: Density of states for spiral state defined by Eq. (B10) for the case of $J = 0.7t$ and $U = 1.1t$. (a) Untwisted state: $(Q_x, Q_y) = (\pi, \pi)$, $\langle \mathcal{H} \rangle / N = -1.391t$. (b) Twisted state: $(Q_x, Q_y) = (0.9\pi, \pi)$, $\langle \mathcal{H} \rangle / N = 1.380t$. As a practical matter, the spiral state represents a domain wall. This traps carriers added to the system the way defects in a semiconductor do, thus causing the system to insulate.

Appendix C: Optical Sum Rule

The f -sum rule for lattice Hamiltonians is widely discussed in the literature, but let us reprise it briefly¹⁶⁶. The buildup of electron density in response to applied potentials is described to linear order by density-density response function

$$\langle \rho_{-\mathbf{q}} \rho_{\mathbf{q}} \rangle = \sum_x | \langle x | \rho_{\mathbf{q}} | 0 \rangle |^2 \frac{2E_x}{(\hbar\omega + i\eta)^2 - E_x^2} \quad (\text{C1})$$

where $|x\rangle$ and $|0\rangle$ are exact excited and ground states of the Hamiltonian \mathcal{H} with energy eigenvalues E_x and $E_0 = 0$, η is an infinitesimal, and

$$\rho_{\mathbf{q}} = \sum_j \sum_{\sigma} \exp(i\mathbf{q} \cdot \mathbf{r}_j) c_{j\sigma}^{\dagger} c_{j\sigma} \quad (\text{C2})$$

The sum rule is

$$\begin{aligned} \int_0^{\infty} \text{Im} \langle \rho_{-\mathbf{q}} \rho_{\mathbf{q}} \rangle \omega d\omega &= -\frac{\pi}{2\hbar^2} \langle 0 | [\rho_{-\mathbf{q}}, [\mathcal{H}, \rho_{\mathbf{q}}]] | 0 \rangle \\ &= -\frac{\pi}{2\hbar^2} \left\{ t \sum_{\langle jk \rangle}^{2N} |e^{i\mathbf{q} \cdot \mathbf{r}_j} - e^{i\mathbf{q} \cdot \mathbf{r}_k}|^2 \sum_{\sigma} (c_{j\sigma}^{\dagger} c_{k\sigma} + c_{k\sigma}^{\dagger} c_{j\sigma}) \right. \\ &\quad \left. - t' \sum_{\langle j\ell \rangle}^{2N} |e^{i\mathbf{q} \cdot \mathbf{r}_j} - e^{i\mathbf{q} \cdot \mathbf{r}_\ell}|^2 \sum_{\sigma} (c_{j\sigma}^{\dagger} c_{\ell\sigma} + c_{\ell\sigma}^{\dagger} c_{j\sigma}) \right\} \end{aligned} \quad (\text{C3})$$

We thus have

$$\lim_{\mathbf{q} \rightarrow 0} \frac{1}{Nq^2b^2} \langle 0 | [\rho_{-\mathbf{q}}, [\mathcal{H}, \rho_{\mathbf{q}}]] | 0 \rangle = 4\chi_{Rt} - 8\chi'_{Rt} \quad (\text{C4})$$

Contact with experiment is made through the in-plane

longitudinal conductivity (in gaussian units)

$$\sigma(\omega) = i\omega \lim_{\mathbf{q} \rightarrow 0} \frac{e^2}{Nab^2q^2} \langle \rho_{-\mathbf{q}} \rho_{\mathbf{q}} \rangle \quad (\text{C5})$$

-
- * R. B. Laughlin: <http://large.stanford.edu>
- ¹ D. A. Bonn, Nat. Phys. **2**, 159 (2006).
 - ² H. Takagi, Nat. Mat. **6**, 179 (2007).
 - ³ D. M. Broun, Nat. Phys. **4**, 170 (2008).
 - ⁴ J. Orenstein and A. Vishwanath, Nat. Phys. **6**, 655 (2010).
 - ⁵ C. M. Varma, Nature (London) **468**, 184 (2010).
 - ⁶ D. N. Basov and A. V. Chubukov, Nat. Phys. **7**, 272 (2011).
 - ⁷ P. Wahl, Nat. Phys. **8**, 514 (2012).
 - ⁸ R. B. Laughlin, Phys. Rev. Lett. **112**, 017004 (2014).
 - ⁹ A. A. Abrikosov, L. P. Gorkov and I. E. Dzyaloshinskii, *Methods of Quantum Field Theory in Statistical Mechanics* (Dover, New York, 1975).
 - ¹⁰ A. L. Fetter and J. D. Walecka, *Quantum Theory of Many-Particle Systems* (McGraw-Hill, New York, 1971).
 - ¹¹ D. Pines and P. Nozières, *Theory of Quantum Liquids: Normal Fermi Liquids* (Perseus, New York, 1989).
 - ¹² S. Chakravarty, R. B. Laughlin, D. K. Morr and C. Nayak, Phys. Rev. B **63**, 094503 (2001).
 - ¹³ C. Nayak and E. Pivovarov, Phys. Rev. B **66**, 064508 (2002).
 - ¹⁴ I. Dimov, P. Goswami, X. Jia and S. Chakravarty, Phys. Rev. B **78**, 134529 (2008).
 - ¹⁵ S. Chakravarty, H.-Y. Kee and C. Nayak, Int. J. Mod. Phys. B **15**, 2901 (2001).
 - ¹⁶ C. Stock, W. J. L. Buyers, Z. Tun, R. Liang, D. Peets, D. Bonn, W. N. Hardy and L. Taillefer, Phys. Rev. B **66**, 024505 (2002).
 - ¹⁷ A. Macridin, M. Jarrell and Th. Maier, Phys. Rev. B **70**, 113105 (2004).
 - ¹⁸ S. Chakravarty and H.-Y. Kee, Proc. Nat. Acad. Sci. U.S.A. **105**, 8835 (2008).
 - ¹⁹ G. J. MacDougall, A. A. Aczel, J. P. Carlo, T. Ito, J. Rodriguez, P. L. Russo, Y. J. Uemura, S. Wakimoto and G. M. Luke, Phys. Rev. Lett. **101**, 017001 (2008).
 - ²⁰ J. G. Bednorz and K. A. Müller, Z. Phys. B **64**, 189 (1986).
 - ²¹ P. W. Anderson and E. Abrahams, Nature London) **327**, 363 (1987).
 - ²² M. K. Wu, J. R. Ashburn, C. J. Torng, P. H. Hor, R. L. Meng, L. Gao, Z. J. Huang, Y. Q. Wang and C. W. Chu, Phys. Rev. Lett. **58**, 908 (1987).
 - ²³ H. Maeda, Y. Tanaka, M. Fukutumi and T. Asano, Jpn. J. Appl. Phys. **27**, L209 (1988).
 - ²⁴ A. Schilling, M. Cantoni, J. D. Guo and H. R. Ott, Nature (London) **363**, 56 (1993).
 - ²⁵ L. F. Mattheiss, Phys. Rev. Lett. **58**, 1028 (1987).
 - ²⁶ A. A. Abrikosov, *Fundamentals of the Theory of Metals* (North-Holland, Amsterdam, 1988).
 - ²⁷ M. L. Cohen and P. W. Anderson, AIP Conf. Proc. **4**, 17 (1972).
 - ²⁸ C. M. Varma, P. B. Littlewood, S. Schmitt-Rink, E. Abrahams and A. E. Ruckenstein, Phys. Rev. Lett. **63**, 1996 (1989).
 - ²⁹ H. Takagi, T. Ido, S. Ishibashi, M. Uota, S. Uchida and Y. Tokura, Phys. Rev. B **40**, 2254 (1989).
 - ³⁰ P. W. Anderson, Science **235**, 1196 (1987).
 - ³¹ M. Cyrot, Nature (London) **330**, 115 (1987).
 - ³² N. F. Mott, Rev. Mod. Phys. **40**, 677 (1968).
 - ³³ P. W. Anderson, *More and Different* (World Scientific, Singapore, 2011), p. 382.
 - ³⁴ A. Schofield, Contemp. Phys. **40**, 95 (1999).
 - ³⁵ G. Stewart, Rev. Mod. Phys. **73**, 797 (2001); **78**, 743 (2006).
 - ³⁶ T. R. Kirkpatrick and D. Belitz, Phys. Rev. Lett. **108**, 086404 (2012).
 - ³⁷ H. C. Jiang, M. S. Block, R. V. Mishmash, J. R. Garrison, D. N. Sheng, O. I. Matrunich and M. P. A. Fisher, Nature (London) **493**, 39 (2013).
 - ³⁸ S. Sachdev, Phys. Rev. Lett. **105**, 151602 (2010).
 - ³⁹ R. Nandkishore, M. A. Metlitski and T. Senthil, Phys. Rev. B **86**, 045128 (2012).
 - ⁴⁰ B. H. Brandow, Adv. Phys. **26**, 651 (1977).
 - ⁴¹ M. R. Norman, Phys. Rev. B **40**, 10632 (1989).
 - ⁴² K. Ohta, R. E. Cohen, K. Hirose, K. Haule, K. Shimizu, and Y. Ohishi, Phys. Rev. Lett. **108**, 026403 (2012).
 - ⁴³ J. C. Slater, J. Appl. Phys. **39**, 761 (1968).
 - ⁴⁴ K. Terakura, A. R. Williams, T. Oguchi and J. Kübler, Phys. Rev. Lett. **52**, 1830 (1984).
 - ⁴⁵ V. I. Anisimov, M. A. Korotin and E. Z. Kurmaev, J. Phys. Condens. Matter **2**, 3973 (1990).
 - ⁴⁶ D. B. McWhan, T. M. Rice and J. P. Remeika, Phys. Rev. Lett. **23**, 1384 (1969).
 - ⁴⁷ H. Nakotte, L. Laughlin, H. Kawanaka, D. N. Argyriou, R. I. Sheldon and Y. Hishihara, J. Appl. Phys. **85**, 4850 (1999).
 - ⁴⁸ M. P. Pasternak, G. K. Rozenberg, G. Y. Machavariani, O. Naaman, R. D. Taylor and R. Jeanloz, Phys. Rev. Lett. **82**, 4663 (1999).
 - ⁴⁹ J. S. Lee, Y. S. Lee, K. W. Kim, T. W. Noh, J. Yu, T. Takeda and R. Kanno, Phys. Rev. B **64**, 165108 (2001).
 - ⁵⁰ J. Park, S.-J. Oh, J.-H. Park, D. M. Kim and C.-B. Eom, Phys. Rev. B **69**, 085108 (2004).
 - ⁵¹ J. R. Patterson, C. M. Aracne, D. D. Jackson, V. Malba, S. T. Weir, P. A. Baker and Y. K. Vohra, Phys. Rev. B **69**, 220101 (2004).
 - ⁵² C. Ulrich, L. J. P. Ament, G. Ghiringhelli, L. Braicovich, M. M. Sala, N. Pezzotta, T. Schmitt, G. Khaliullin, J. van den Brink, H. Roth, T. Lorenz and B. Keimer, Phys. Rev. Lett. **103**, 107205 (2009).
 - ⁵³ H. D. Zhou, Y. J. Jo, J. Fiore Carpino, G. J. Munoz, C. R. Wiebe, J. G. Cheng, F. Rivadulla and D. T. Adroja, Phys. Rev. B **81**, 212401 (2010).
 - ⁵⁴ M. Imada, A. Fujimori and Y. Tokura, Rev. Mod. Phys. **70**, 1039 (1998).
 - ⁵⁵ S. Sachdev, Rev. Mod. Phys. **75**, 913 (2003).

- ⁵⁶ P. A. Lee, N. Nagaosa and X.-G. Wen, *Rev. Mod. Phys.* **78**, 17 (2006).
- ⁵⁷ T. Senthil and P. A. Lee, *Phys. Rev. Lett.* **103**, 076402 (2009).
- ⁵⁸ F. Gebhard, *The Mott Metal-Insulator Transition: Models and Methods* (Springer, Heidelberg, 2010).
- ⁵⁹ P. W. Anderson, P. A. Lee, M. Randeria, T. M. Rice, N. Trividi and F. C. Zhang, *J. Phys. Condens. Matter* **16**, R755 (2004).
- ⁶⁰ J. K. Jain and P. W. Anderson, *Proc. Nat. Acad. Sci. U.S.A.* **106**, 9131 (2009).
- ⁶¹ R. B. Laughlin, *Philos. Mag.* **86**, 1165 (2006).
- ⁶² E. Dagotto, *Rev. Mod. Phys.* **66**, 763 (1994).
- ⁶³ T. A. Maier, M. Jarrell and D. J. Scalapino, *Phys. Rev. B* **74**, 094513 (2006).
- ⁶⁴ B. Edegger, V. N. Muthukumar and C. Gros, *Adv. Phys.* **56**, 927 (2007).
- ⁶⁵ P. W. Leung, *Int. J. Mod. Phys. B* **21**, 3118 (2007).
- ⁶⁶ A. G. Sun, D. A. Gajewski, M. B. Maple and R. C. Dynes, *Phys. Rev. Lett.* **72**, 2267 (1994).
- ⁶⁷ S. A. Kivelson, D. S. Rokhsar and J. P. Sethna, *Europhys. Lett.* **6**, 353 (1988).
- ⁶⁸ A. Damascelli, Z. Hussain and Z.-X. Shen, *Rev. Mod. Phys.* **75**, 473 (2003).
- ⁶⁹ P. Monthoux, A. V. Balatsky and D. Pines, *Phys. Rev. Lett.* **67**, 3448 (1991).
- ⁷⁰ P. B. Littlewood and C. M. Varma, *Phys. Rev. B* **46**, 405 (1992).
- ⁷¹ D. A. Wollman, D. J. Van Harlingen, W. C. Lee, D. M. Ginsberg and A. J. Leggett, *Phys. Rev. Lett.* **71**, 2134 (1993).
- ⁷² D. J. Scalapino, *Phys. Rep.* **250**, 329 (1995).
- ⁷³ C. C. Tsuei and J. R. Kirtley, *Rev. Mod. Phys.* **72**, 969 (2000).
- ⁷⁴ M. Platié, J. D. F. Mottershead, I. S. Elfimov, D. C. Peets, R. Liang, D. A. Bonn, W. N. Hardy, S. Chiuzaibaian, M. Falub, M. Shi, L. Patthey and A. Damascelli, *Phys. Rev. Lett.* **95**, 077001 (2005).
- ⁷⁵ J. M. Luttinger, *Phys. Rev.* **119**, 1153 (1960).
- ⁷⁶ N. E. Hussey, M. Abdel-Jawad, A. Carrington, A. P. Mackenzie and L. Balices, *Nature (London)* **425**, 814 (2003).
- ⁷⁷ S. E. Sebastian, N. Harrison and G. G. Lonzarich, *Philos. Trans. R. Soc. London Ser. A* **369**, 1687 (2011).
- ⁷⁸ B. Vignolle, D. Vignolles, D. LeBoeuf, S. Lepault, B. Ramshaw, R. Liang, D. A. Bonn, W. N. Hardy, N. Diron-Leyraud, A. Carrington, N. E. Hussey, L. Taillefer and C. Proust, *C. R. Physique* **12**, 446 (2011).
- ⁷⁹ H. Takagi, B. Batlogg, H. L. Kao, J. Kwo, R. J. Cava, J. J. Krajewski and W. F. Peck, Jr., *Phys. Rev. Lett.* **69**, 2975 (1992).
- ⁸⁰ X. F. Sun, K. Segawa and Y. Ando, *Phys. Rev. Lett.* **93**, 107001 (2004).
- ⁸¹ J. Zaanen and B. Hosseinkhani, *Phys. Rev. B* **70**, 060509 (2004).
- ⁸² M. R. Norman, D. Pines and C. K. Kallin, *Adv. Phys.* **54**, 715 (2005).
- ⁸³ S. E. Sebastian, N. Harrison, M. M. Altarawneh, C. H. Mielke, R. Liang, D. A. Bonn, W. N. Hardy and G. G. Lonzarich, *Proc. Nat. Acad. Sci. U.S.A.* **107**, 6175 (2010).
- ⁸⁴ N. P. Butch, K. Jin, K. Kirshenbaum, R. L. Greene and J. Paglione, *Proc. Nat. Acad. Sci.* **109**, 8440 (2012).
- ⁸⁵ C. M. Varma, *Phys. Rev. Lett.* **83**, 3538 (1999).
- ⁸⁶ S. Sachdev, *Phys. Status Solidi B* **247**, 537 (2010).
- ⁸⁷ S. Chakravarty, *Rep. Prog. Phys.* **74**, 022501 (2011).
- ⁸⁸ T. Timusk and B. Statt, *Rep. Prog. Phys.* **62**, 61 (1999).
- ⁸⁹ A. G. Loeser, Z.-X. Shen, D. S. Dessau, D. S. Marshall, C. H. Park, P. Fournier and A. Kapitulnik, *Science* **273**, 325 (1996).
- ⁹⁰ M. Le Tacon, A. Sacuto, A. Georges, G. Kotliar, Y. Gallais, D. Colson and A. Forget, *Nat. Phys.* **2**, 537 (2006).
- ⁹¹ N. Doiron-Leyraud, C. Proust, D. LeBoeuf, J. Levallois, J.-B. Bonnemaïson, R. Liang, D. A. Bonn, W. A. Hardy and L. Taillefer, *Nature (London)* **447**, 565 (2007).
- ⁹² B. Valenzuela and E. Bascones, *Phys. Rev. Lett.* **98**, 227002 (2007).
- ⁹³ I. M. Vishik, M. Mashimoto, R.-H. He, W.-S. Lee, F. Schmitt, D. Lu, R. G. Moore, C. Zhang, W. Meevasana, T. Sasagawa, S. Uchida, K. Fujita, S. Ichida, M. Ishikado, Y. Yoshida, H. Eisaki, Z. Hussain, T. P. Devereaux and Z.-X. Shen, *Proc. Nat. Acad. Sci. U.S.A.* **109**, 18332 (2012).
- ⁹⁴ M. Vojta and O. Rösch, *Phys. Rev. B* **77**, 094504 (2008).
- ⁹⁵ Y. Kohsaka, T. Hanaguri, M. Azuma, M. Takano, J. C. Davis and H. Takagi, *Nat. Phys.* **8**, 534 (2012).
- ⁹⁶ K. McElroy, D.-H. Lee, J. E. Hoffman, K. M. Lang, J. Lee, E. W. Hudson, H. Eisaki, S. Uchida and J. C. Davis, *Phys. Rev. Lett.* **94**, 197005 (2005).
- ⁹⁷ I. Affleck, Z. Zou, T. Hsu and P. W. Anderson, *Phys. Rev. B* **38**, 745 (1988).
- ⁹⁸ S. Liang and N. Trivedi, *Phys. Rev. Lett.* **64**, 232 (1990).
- ⁹⁹ H. A. Mook, P. Dai, S. M. Hayden, A. Hiess, J. W. Lynn, S.-H. Lee and F. Dogan, *Phys. Rev. B* **66**, 144513 (2002); H. A. Mook, P. Dai, S. M. Hayden, A. Hiess, S.-H. Lee and F. Dogan, *ibid.* **69**, 134509 (2004).
- ¹⁰⁰ T. M. Rice, K.-Y. Yang and F. C. Zhang, *Rep. Prog. Phys.* **75**, 016502 (2012).
- ¹⁰¹ D. F. Schroeter and S. Doniach, *Phys. Rev. B* **69**, 094407 (2004).
- ¹⁰² C. M. Varma, *Phys. Rev. B* **61**, 3804 (2000); **73**, 155113 (2006).
- ¹⁰³ Y. He and C. M. Varma, *Phys. Rev. B* **85**, 155102 (2012).
- ¹⁰⁴ B. Fauqué, Y. Sidis, V. Hinkov, S. Pailhès, C. T. Lin, X. Chaud and P. Bourges, *Phys. Rev. Lett.* **96**, 197001 (2006).
- ¹⁰⁵ H. A. Mook, Y. Sidis, B. Fauqué, V. Balédent and P. Bourges, *Phys. Rev. B* **78**, 020506 (2008).
- ¹⁰⁶ J. E. Sonier, V. Pacradouni, S. A. Sabok-Sayr, W. N. Hardy, D. A. Bonn, R. Liang and H. A. Mook, *Phys. Rev. Lett.* **103**, 167002 (2009).
- ¹⁰⁷ Y. Li, V. Balédent, G. Yu, N. Bašić, K. Hradil, R. A. Mole, Y. Sidis, P. Steffens, X. Zhao, P. Bourges and M. Greven, *Nature (London)* **468**, 283 (2010).
- ¹⁰⁸ P. Bourges and Y. Sidis, *C. R. Phys.* **12**, 461 (2011).
- ¹⁰⁹ S. Strässle, B. Graneli, M. Mali, J. Roos and H. Keller, *Phys. Rev. Lett.* **106**, 097003 (2011).
- ¹¹⁰ S. Lederer and S. A. Kivelson, *Phys. Rev. B* **85**, 155130 (2012).
- ¹¹¹ R. Shankar, *Rev. Mod. Phys.* **66**, 129 (1994).
- ¹¹² S. L. Sondhi, S. M. Girvin, J. P. Carini and D. Shahar, *Rev. Mod. Phys.* **69**, 315 (1997).
- ¹¹³ P. W. Anderson, *Phys. Rev. Lett.* **18**, 1049 (1967).
- ¹¹⁴ P. W. Anderson, *Rev. Math. Phys.* **06**, 1085 (1994).
- ¹¹⁵ J. R. Schrieffer, *Theory of Superconductivity* (Benjamin Cummings, New York, 1983).
- ¹¹⁶ D. Belitz, T. R. Kirkpatrick and T. Vojta, *Rev. Mod. Phys.* **77**, 579 (2005).
- ¹¹⁷ A. A. Abrikosov and I. M. Khalatnikov, *Rep. Prog. Phys.* **22**, 329 (1959).

- ¹¹⁸ P. Nozières and J. M. Luttinger, Phys. Rev. **127**, 1423 (1962).
- ¹¹⁹ P. Wölfle, Z. Phys. **232**, 38 (1970).
- ¹²⁰ N. Dupuis and G. Y. Chitov, Phys. Rev. B **54**, 3040 (1996).
- ¹²¹ I. M. Vishik, W. S. Lee, R.-H. He, M. Hashimoto, Z. Husain, T. P. Devereaux and Z.-X. Shen, New J. Phys. **12**, 105008 (2010).
- ¹²² P. D. Johnson, T. Valla, A. V. Fedorov, Z. Yusof, B. O. Wells, Q. Li, A. R. Moodenbaugh, G. D. Gu, N. Koshizuka, C. Kendziora, S. Jian and D. G. Hinks, Phys. Rev. Lett. **87**, 177007 (2001).
- ¹²³ N. P. Armitage, D. H. Lu, C. Kim, A. Damascelli, K. M. Shen, F. Ronning, D. L. Feng, P. Bogdanov, Z.-X. Shen, Y. Onose, Y. Taguchi, Y. Tokura, P. K. Mang, N. Kaneko and M. Greven, Phys. Rev. Lett. **87**, 147003 (2001).
- ¹²⁴ E. Pavarini, I. Dasgupta, T. Saha-Dasgupta, O. Jepsen and O. K. Andersen, Phys. Rev. Lett. **87**, 047003 (2001).
- ¹²⁵ H. J. Schulz, Phys. Rev. Lett. **64**, 1445 (1990).
- ¹²⁶ M. Inui and P. B. Littlewood, Phys. Rev. B **44**, 4415 (1991).
- ¹²⁷ F. Hu, S. K. Sarker and C. Jayaprakash, Phys. Rev. B **50**, 17901 (1994).
- ¹²⁸ A. V. Chubukov and K. A. Musaelian, Phys. Rev. B **51**, 12605 (1995).
- ¹²⁹ J. Li, H. Lin and C.-D. Gong, Solid State Commun. **115**, 449 (2000).
- ¹³⁰ P. W. Anderson, Phys. Rev. **115**, 2 (1959).
- ¹³¹ D. J. Scalapino, “Numerical studies of the 2D Hubbard Model,” in *Handbook of High-Temperature Superconductivity*, edited by J. R. Schrieffer and J. S. Brooks (Springer, Heidelberg, 2007), p. 495.
- ¹³² K. Yamada, E. Kudo, Y. Endoh, Y. Hidaka, M. Oda, M. Suzuki and T. Murakami, Solid State Commun. **64**, 753 (1987).
- ¹³³ D. Vaknin, S. K. Sinha, C. Stassis, L. L. Miller and D. C. Johnston, Phys. Rev. B **41**, 1926 (1990).
- ¹³⁴ L. P. Regnault, Ph. Bourges and P. Burlet, “Phase Diagrams and Spin Correlations in $\text{YBa}_2\text{Cu}_3\text{O}_{6+x}$,” in *Neutron Scattering in Layered Copper-Oxide Superconductors*, edited by A. Furrer (Kluwer, Amsterdam, 1998), p. 90.
- ¹³⁵ J. Tranquada, “Neutron Scattering Studies of Antiferromagnetic Correlations in Cuprates,” in *Handbook of High-Temperature Superconductivity*, edited by J. R. Schrieffer and J. S. Brooks (Springer, New York, 2007), p. 257.
- ¹³⁶ E. Demler, W. Hanke and S.-C. Zhang, Rev. Mod. Phys. **76**, 909 (2004).
- ¹³⁷ S. Hufner, M. A. Hossain, A. Damascelli and G. A. Sawatsky, Rep. Prog. Phys. **71**, 062501 (2008).
- ¹³⁸ H. Ding, J. R. Engelbrecht, Z. Wang, J. C. Campuzano, S.-C. Wang, H.-B. Yang, R. Rogan, T. Takahashi, K. Kadowaki and D. G. Hinks, Phys. Rev. Lett. **87**, 227001 (2001).
- ¹³⁹ D. C. Peets, J. D. F. Motterhead, B. Wu, I. S. Elfimov, R. Liang, W. N. Hardy, D. A. Bonn, M. Paudsepp, N. J. C. Ingle and A. Damascelli, New J. Phys. **9**, 28 (2007).
- ¹⁴⁰ F. Venturini, M. Opel, R. Hackl, H. Berger, L. Forró and B. Revaz, J. Phys. Chem. Solids **63**, 2345 (2002).
- ¹⁴¹ S. Sugai, H. Suzuki, Y. Takayanagi, T. Hosokawa and N. Hayamizu, Phys. Rev. B **68**, 184504 (2003).
- ¹⁴² J. F. Zasadzinski, L. Ozyuzer, N. Miyakawa, K. E. Gray, D. G. Hinks and C. Kendziora, Phys. Rev. Lett. **87**, 067005 (2001).
- ¹⁴³ Y. Sidis, S. Pailhès, B. Keimer, P. Bourges, C. Ulrich and L. P. Regnault, Phys. Status Solidi B **241**, 1204 (2004).
- ¹⁴⁴ H. He, P. Bourges, Y. Sidis, C. Ulrich, L. P. Regnault, S. Pailhès, N. S. Berzigiarova, N. N. Kolesnikov and B. Keimer, Science **295**, 1045 (2002).
- ¹⁴⁵ D. G. Hawthorn, S. Y. Li, M. Sutherland, E. Boaknin, R. W. Hill, C. Proust, F. Ronning, M. A. Tanatar, J. Paglione, L. Taillefer, D. Peets, R. Liang, D. A. Bonn, W. N. Hardy and N. N. Kolesnikov, Phys. Rev. B **75**, 104518 (2007).
- ¹⁴⁶ M. Sutherland, D. G. Hawthorn, R. W. Hill, F. Ronning, S. Wakimoto, H. Zhang, C. Proust, E. Boaknin, C. Lupien, L. Taillefer, R. Liang, D. A. Bonn, W. N. Hardy, R. Gagnon, N. E. Hussey, T. Kimura, M. Nohara and H. Takagi, Phys. Rev. B **67**, 174520 (2003).
- ¹⁴⁷ G. Deutscher, Nature (London) **397**, 411 (1999); Rev. Mod. Phys. **77**, 109 (2005).
- ¹⁴⁸ R. S. Gonnelli, A. Calzolari, D. Daghero, L. Natale, G. A. Ummarino, V. A. Stepanov and M. Ferretti, J. Phys. Chem. Solids **63**, 2369 (2002).
- ¹⁴⁹ J. L. Tallon, F. Barber, J. G. Storey and J. W. Loram, Phys. Rev. B **87**, 140508 (2013); J. L. Tallon, J. W. Loram, J. R. Cooper, C. Panagopoulos and C. Bernhard, *ibid.*, **68**, 180501 (2003).
- ¹⁵⁰ C. Bernhard, J. L. Tallon, T. Blasius, A. Golnik and C. Niedermayer, Phys. Rev. Lett. **86**, 1614 (2001).
- ¹⁵¹ T. Pereg-Barnea, P. J. Turner, R. Harris, G. K. Mullins, J. S. Bobowski, M. Raudsepp, R. Liang, D. A. Bonn and W. N. Hardy, Phys. Rev. B **69**, 184513 (2004).
- ¹⁵² W. Yu, J. S. Higgins, P. Bach and R. L. Greene, Phys. Rev. B **76**, 020503 (2007).
- ¹⁵³ H. L. Luo, S. Y. Ding and X. S. Wu, J. Appl. Phys. **89**, 7663 (2001).
- ¹⁵⁴ S. Uchida, T. Ido, H. Takagi, T. Arima, Y. Tokura and S. Tajima, Phys. Rev. B **43**, 7942 (1991).
- ¹⁵⁵ W. J. Padilla, Y. S. Lee, M. Dumm, G. Blumberg, S. Ono, K. Segawa, S. Komiya, Y. Ando and D. N. Basov, Phys. Rev. B **72**, 060511 (2005).
- ¹⁵⁶ V. J. Emery and S. A. Kivelson, Nature (London) **374**, 434 (1995).
- ¹⁵⁷ L. Benfatto, C. Castellani and T. Giamarchi, Phys. Rev. Lett. **98**, 117008 (2007).
- ¹⁵⁸ S. Wakimoto, R. J. Birgeneau, M. A. Kastner, Y. S. Lee, R. Erwin, P. M. Gehring, S. H. Lee, M. Fujita, K. Yamada, Y. Endoh, K. Hirota and G. Shirane, Phys. Rev. B **61**, 3699 (2000).
- ¹⁵⁹ B. Keimer, R. J. Birgeneau, A. Cassenko, Y. Endoh, M. Greven, M. A. Kastner and G. Shirane, Z. Phys. B **91**, 373 (1993).
- ¹⁶⁰ A. V. Chubukov and D. M. Frenkel, Phys. Rev. B **46**, 11884 (1992).
- ¹⁶¹ H. Nakanishi, Prog. Theor. Phys. **72**, 967 (1984).
- ¹⁶² R. Coldea, S. M. Hayden, G. Aeppli, T. G. Perring, C. D. Frost, T. E. Mason, S.-W. Cheong and Z. Fisk, Phys. Rev. Lett. **86**, 5377 (2001).
- ¹⁶³ N. Harima, J. Matsuno, A. Fujimori, Y. Onose, Y. Taguchi, and Y. Tokura, Phys. Rev. B **64**, 220507 (2001).
- ¹⁶⁴ M. Ikeda, M. Takizawa, T. Yoshida, A. Fujimori, K. Segawa and Y. Ando, Phys. Rev. B **82**, 020503 (2010).
- ¹⁶⁵ Y. Nagaoka, Prog. Theor. Phys. **52**, 1716 (1974).
- ¹⁶⁶ H. Monien and K. S. Bedell, Phys. Rev. B **45**, 3164 (1992).